International Journal of Endocrinology

Novel Insights into Adrenal Disorders

Lead Guest Editor: Rosa M. Paragliola
Guest Editors: Salvatore M. Corsello and Giampaolo Papi

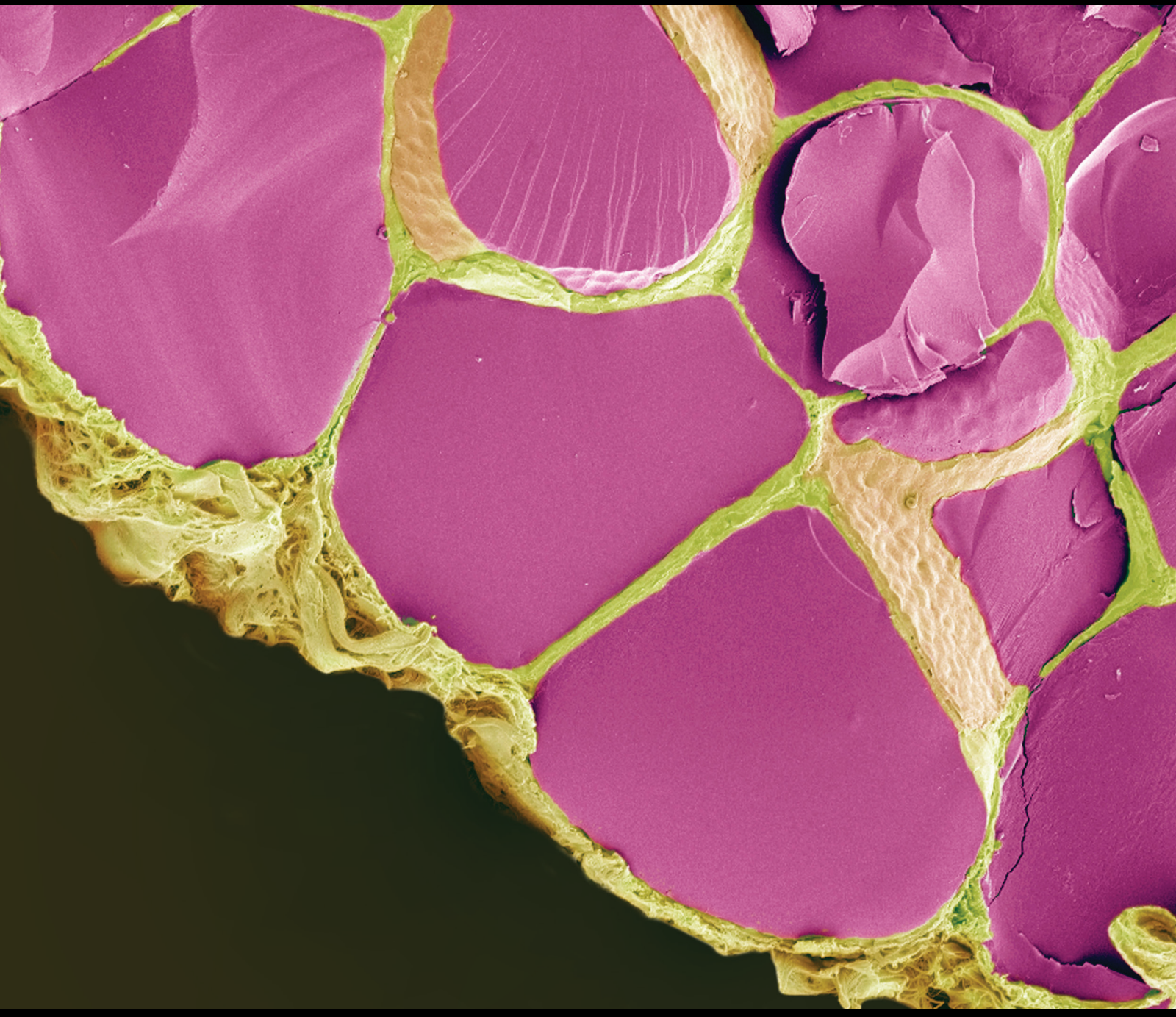

Novel Insights into Adrenal Disorders

International Journal of Endocrinology

Novel Insights into Adrenal Disorders

Lead Guest Editor: Rosa M. Paragliola
Guest Editors: Salvatore M. Corsello and Giampaolo Papi

Contents

Hindawi
International Journal of Endocrinology
Volume 2019, Article ID 2860810, 6 pages
https://doi.org/10.1155/2019/2860810

Research Article

The Value of Adrenal Androgens for Correcting Cortisol Lateralization in Adrenal Venous Sampling in Patients with Normal Cortisol Secretion

Wenjing Zhang,[1] Keying Zhu,[1] Hongyun Li,[1] Yan Zhang,[1] Dalong Zhu,[1] Xuebin Zhang,[2] and Ping Li[1]

[1]*Department of Endocrinology, Drum Tower Hospital Affiliated to Nanjing University Medical School, Nanjing 210008, China*
[2]*Department of Imaging, Drum Tower Hospital Affiliated to Nanjing University Medical School, Nanjing 210008, China*

Correspondence should be addressed to Xuebin Zhang; xuebinm@hotmail.com and Ping Li; li78321@yeah.net

Received 6 March 2019; Accepted 17 June 2019; Published 31 July 2019

Guest Editor: Giampaolo Papi

The management of patients with adrenocorticotropic hormone-independent Cushing's syndrome and bilateral adrenal masses is challenging. Adrenal venous sampling (AVS) has been used to identify functional lesions in previous studies, but it is not always reliable. The present study aims to address the variability of cortisol in the adrenal veins of patients without excessive cortisol secretion and investigate the use of adrenal androgens to correct the cortisol lateralization ratio in AVS. Thirty-seven patients with primary aldosteronism underwent successful AVS. Patients with normal cortisol secretion exhibited a wide range of cortisol concentrations in the right (601-89, 400 nmol/l) and left (331-35, 300 nmol/l) adrenal veins. The median cortisol gradients between adrenal venous and peripheral venous samples were 15.25 and 10.14 in the right and left sides, respectively, and the cortisol lateralization ratio (high side to low side) was as high as 9.49 (median 1.54). The mean plasma levels of cortisol in the adrenal venous and peripheral venous samples decreased from t-15 to t0. Significant positive correlations were observed between the cortisol concentrations and both androstenedione and dehydroepiandrosterone concentrations in the right and left adrenal veins. After correcting for androstenedione or dehydroepiandrosterone levels, the cortisol lateralization ratio was less than 2 in most adrenal venous samples. The present study demonstrated the wide variation in cortisol concentrations in the adrenal veins of patients with normal cortisol secretion. The adrenal androgens might be ideal analytes used as normalizers when assessing the cortisol lateralization of AVS in normal or hypercortisolism cases.

1. Introduction

Adrenocorticotropic hormone (ACTH)-independent Cushing's syndrome (CS) is occasionally caused by bilateral adrenocortical lesions. Such patients may have a unilateral cortisol-secreting adenoma with a contralateral nonfunctioning cortical adenoma, bilateral cortisol-secreting adenomas, or bilateral ACTH-independent macronodular adrenal hyperplasia (AIMAH) mimicking bilateral single adenomas [1]. Compared to the management of adrenal CS in patients with a unilateral cortical adenoma, management of ACTH-independent CS in patients with bilateral adrenal masses is problematic [2]. It is critical during treatment decision making to differentiate between a functioning or nonfunctioning adrenal cortical mass and to distinguish the unilateral overproduction of cortisol from bilateral disease.

Adrenal venous sampling (AVS) has been successfully used to lateralize the source of aldosterone hypersecretion in patients with primary aldosteronism [3, 4]. Several previous studies have reported using AVS for evaluation of cortisol-producing adrenal masses [1, 5–7]. Although it is helpful in some cases, this procedure is not successful in all cases [8–10]. Thus, it is still necessary to validate the protocol and identify the underlying factors that affect the interpretation of the results.

According to the literature and our experience using AVS in primary aldosteronism (PA) cases, the following factors might interfere with the assessment of lateralization

in ACTH-independent CS: (1) a stress reaction involving increased cortisol release, (2) fluctuating levels of cortisol induced by ACTH secretion, and (3) different dilutional effects in the right and left adrenals due to the adrenal venous (AV) anatomy [11]. However, few studies have addressed the effect of cortisol variation in normal AV samples [12, 13]. Furthermore, no consensus has been reached on the optimal parameters that can be used in hypercortisolism cases to correct for the cortisol gradient between the right and left adrenals caused by the above factors.

The adrenal androgens androstenedione and dehydroepiandrosterone (DHEA) are mainly produced in the zona reticularis. Recently published studies from our group and others suggested that adrenal androgens are useful for assessing the selectivity of AVS in PA [14–16]. The present study aims to investigate the variation of cortisol in AVS in patients with normal cortisol secretion. Furthermore, we aim to determine whether adrenal androgens are useful in correcting for the side-to-side gradient of cortisol caused by physiologic factors or anatomic differences.

2. Subjects and Methods

2.1. Subjects. We consecutively recruited PA patients undergoing AVS among patients referred to the endocrinology department at our hospital for suspected secondary hypertension. The diagnosis of PA was confirmed by an intravenous saline infusion or a captopril test. A 1 mg dexamethasone suppression test (DST) was performed to exclude autonomous cortisol secretion, indicated by a post-DST cortisol level less than 50 nmol/l. We performed twenty-four-hour urinary catecholamine measurement to exclude pheochromocytoma. Patients were offered AVS according to the guidelines of the US Endocrine Society [17]. Informed written consent was obtained from each participant. All procedures were performed in accordance with the principles of the Declaration of Helsinki and institutional guidelines.

2.2. AVS Procedure. AVS was performed as described previously [15]. The procedure was conducted between 0800 and 1200 hours by one radiologist using a bilateral simultaneous technique without cosyntropin stimulation. Blood was collected by gravity or with gentle negative pressure. Intraprocedural plasma cortisol concentration (PCC) measurement was performed to confirm correct catheter placement during AVS. In 17 patients, blood samples were collected twice at baseline, with a 15 min interval between time -15 and 0 (t-15 and t0). During this interval, the catheter remained in the adrenal vein on both sides. Heparin was injected intravenously to avoid the risk of thrombosis. Another portion of the sample was stored at 80°C for later measurement of adrenal androgens. Finally, 37 consecutive patients who underwent a total of 54 successful AVS procedures were included.

2.3. Measurements of Cortisol, Androstenedione, and DHEA. The PCC was measured with a commercially available kit (Immulite 2000 Cortisol, Siemens Healthcare Diagnostics Products Limited, Gwynedd LL55 4EL, United Kingdom). The intra- and interassay coefficients of variation (CVs) for PCCs were 4.6% and 6.8%, respectively. The plasma concentrations of androstenedione and DHEA were measured using a commercial ELISA kit (DRG International, Inc., USA). The intra-assay CVs for androstenedione ranged from 0.35% for high plasma concentrations to 1.50% for low concentrations. The interassay CVs for DHEA ranged from 0.71% for high plasma concentrations to 2.85% for low concentrations. The intra-assay and interassay CVs for this assay were 5.2% and 9.8%, respectively.

2.4. Statistical Analysis. Data are expressed as the means and SDs or, in the case of skewed distributions, as medians and ranges. Kruskal-Wallis and Mann-Whitney U tests were used to assess the significance of differences in variables at the three sampling sites or between groups. Relationships among cortisol, androstenedione, and DHEA were assessed by one-tailed Spearman's correlation coefficient (r_s). A paired t test was used to compare the log-transformed values obtained at t-15 and t0. A value of $P < 0.05$ was considered significant [15]. SPSS 18.0 for Windows and GraphPad Prism 4.0 were used for the analysis.

3. Results

3.1. AV Cortisol and Adrenal Androgen Levels and Cortisol Lateralization. Patients with normal cortisol secretion exhibited a wide range of cortisol concentrations in the right (601-89, 400 nmol/l) and left (331-35, 300 nmol/l) adrenal veins. The median cortisol gradients between AV and peripheral venous (PV) samples were 15.25 and 10.14 on the right and left sides, respectively. Consistent with the cortisol concentrations, considerably higher plasma androstenedione and DHEA concentrations were detected in the right and left AV samples than in PV samples ($P < 0.01$). The androstenedione and DHEA gradients between AV and PV samples were approximately 2-3 times higher than those of cortisol. Although no significant difference was observed in cortisol levels between the right and left adrenal veins, the cortisol lateralization (high-side to low-side) was as high as 9.49 (median 1.54). Similar findings were also observed for androstenedione and DHEA (Table 1).

3.2. Variation in Plasma Cortisol Levels over Time. To investigate the variation of hormones over time, we measured cortisol levels in repeated samples from 17 PA patients obtained at 15 min intervals as described previously [15]. The mean plasma levels of cortisol in the AV and PV samples decreased from t-15 to t0. Compared to t-15, the AV cortisol levels on the right side were significantly decreased at t0 [$P < 0.05$, 7860 (4260-11, 360) nmol/l vs. 3920 (1515-9120) nmol/l]. However, cortisol concentrations in the left AV samples exhibited a nonsignificant decrease from t-15 to t0 [5600 (2780-9945) nmol/l vs. 3420 (1632-7665) nmol/l]. The plasma cortisol levels in the left and right AV samples decreased by 61% and 64%, respectively. As a result, the cortisol gradients between the AV and PV samples also decreased from t-15

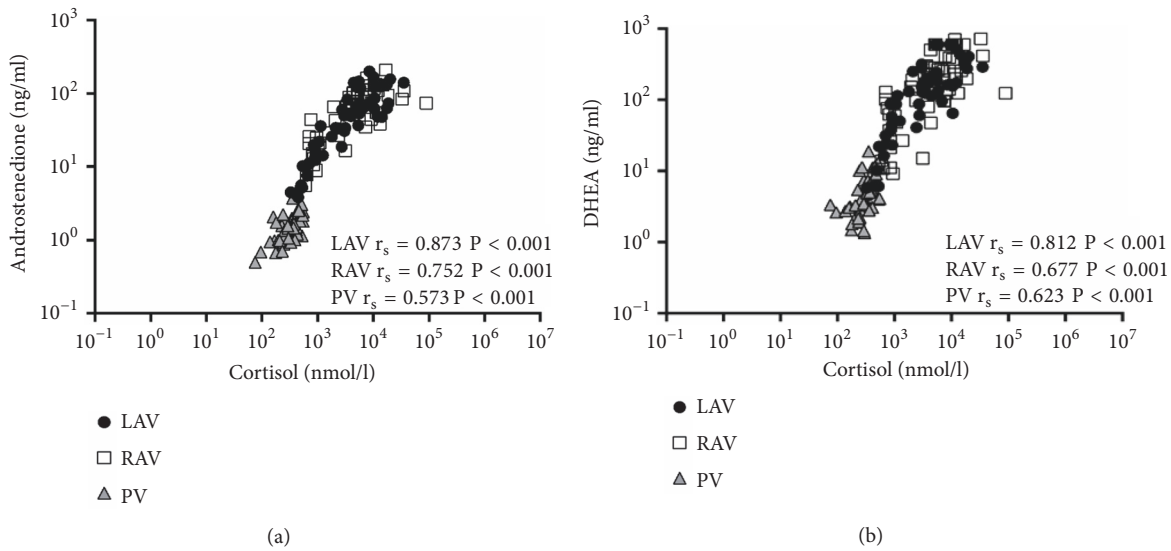

Figure 1: Correlations among plasma androstenedione (a), plasma DHEA (b), and plasma cortisol levels for AVS. LAV, left adrenal vein; RAV, right adrenal vein; and PV, peripheral vein.

Table 1: Adrenal vein cortisol and adrenal androgen measurements in patients with normal cortisol secretion undergoing adrenal venous sampling [M (25-75%)].

Parameter	LAV (range)	RAV (range)	PV (range)	LAV/PV	RAV/PV	Lateralization ratio [A] (range)
Cortisol (nmol/l)	3270 * (331-35300)	4695 * (601-89400)	317 (75-557)	10.14 (1.57-88.21)	15.25 (2.01-206.47)	1.54 (1.00-9.49)
Androstenedione (ng/ml)	48.65 * (3.87-200.00)	66.69 * (5.57-210.21)	1.51 (0.50-3.76)	27.62 (2.52-169.34)	43.01 (6.84-129.30)	1.49 (1.00-14.91)
DHEA (ng/ml)	132.74 * (5.81-616.43)	160.14 * (9.14-722.21)	4.24 (1.34-18.99)	35.76 (1.83-291.26)	46.05 (2.60-243.67)	1.69 (1.00-22.52)

DHEA, dehydroepiandrosterone; LAV, left adrenal vein; RAV, right adrenal vein; and PV, peripheral vein.
* P < 0.01, vs. PV; [A] side-to-side (high-side to low-side) adrenal vein hormone gradient.

to t0. The cortisol lateralization did not change significantly from t-15 to t0 (1.69 vs. 1.51) (Table 2).

3.3. Correlations between Cortisol and Adrenal Androgens. Significant positive correlations were observed between the cortisol concentrations and both androstenedione and DHEA concentrations in the right (r_s = 0.752 and 0.677, P < 0.001, resp.) and left (r_s = 0.873 and 0.812, P < 0.001, resp.) AV samples (Figures 1(a) and 1(b)).

3.4. Cortisol Lateralization Ratio after Correction for Adrenal Androgens. Among 54 AVS procedures, 35 AVS procedures exhibited a cortisol lateralization ratio (high-side to low-side) less than 2 between the right and left AV samples, and 19 AVS procedures had a ratio greater than 2. After correction for androstenedione levels, only 4 AVS procedures had a lateralization ratio greater than 2. After correction for DHEA, 9 AVS procedures had a lateralization ratio greater than 2 (Figure 2).

4. Discussion

These data from patients without excessive cortisol secretion undergoing AVS demonstrated that adrenal vein cortisol concentrations exhibit great variation, including significant variation in the plasma cortisol levels over time and the cortisol gradient between the right and left adrenal veins. Furthermore, we confirmed that the adrenal androgens androstenedione and DHEA are useful in correcting for the side-to-side gradient of cortisol.

The optimum surgical treatment of ACTH-independent CS and subclinical CS is less clear when a patient appears to have bilateral adrenal cortical adenomas [2]. Bilateral adrenalectomy can resolve the condition but results in postoperative adrenal insufficiency, necessitating lifelong glucocorticoid and mineralocorticoid replacement [1, 2]. Therefore, it is necessary to differentiate among bilateral cortisol-secreting adenomas, unilateral cortisol-secreting adenoma, and nonfunctional adenomas and to identify the lesion to resect.

Table 2: Plasma cortisol levels in the adrenal veins measured from repeated samples (t-15, t0) during AVS [M (25-75%)].

Parameter	LAV (range)	RAV (range)	PV (range)	LAV/PV	RAV/PV	Lateralization ratio [A] (range)
Cortisol (nmol/l) t-15	5600 (2780-9945)	7860 (4260-11360)	309 (247-457)	18.22 (1.97-40.82)	24.39 (3.44-206.47)	1.69 (1.02-5.14)
Cortisol (nmol/l) t0	3420 (1632-7665)	3920 (1515-9120)	292 (234-391)	10.76 (2.16-88.21)	13.42 (2.01-65.50)	1.51 (1.00-6.22)
P (t-15 vs t0)	0.455	0.035	0.082	0.209	0.654	0.904
Variance ratio (t0–t-15/t-15)	0.61±0.51	0.64±0.37	0.17±0.16			

LAV, left adrenal vein; RAV, right adrenal vein; and PV, peripheral vein. [A] side-to-side (high-side to low-side) adrenal vein cortisol gradient.

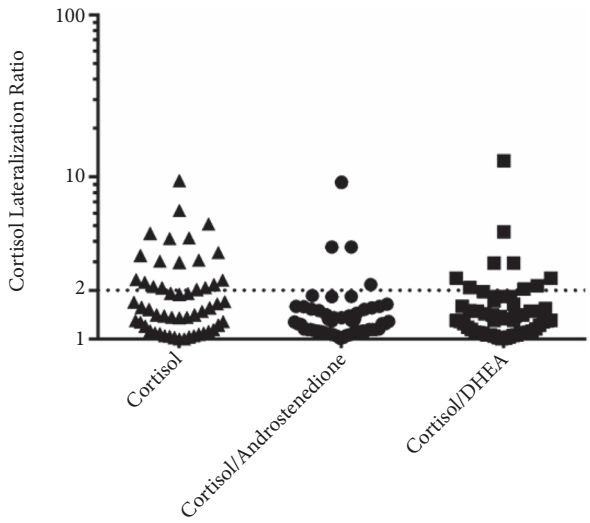

Figure 2: High-side to low-side adrenal vein cortisol concentration ratios with or without adrenal androgens correction. AV, adrenal vein.

AVS is commonly used to distinguish the source of hormonal production in patients with primary hyperaldosteronism [3]. Several studies have reported the use of AVS for CS with bilateral masses, of which the most well-known study was conducted by the Mayo Clinic (Rochester, MN, USA) [18]. Young reported ten patients with bilateral adrenal masses and ACTH-independent CS or subclinical CS who underwent AVS. According to the results, a cortisol AV: PV gradient of 6.5 was consistent with a cortisol-secreting adenoma. If the ratio was ≤ 3.3, the lesion was considered a nonfunctional adenoma, and when the bilateral adrenal vein lateralization ratio was ≤ 2.0, the condition was considered bilateral cortisol hypersecretion [18].

Subsequent studies followed the criteria of Young in interpreting the results of AVS in patients with bilateral adrenal masses and ACTH-independent CS. However, AVS has not always been reliable in differentiating the source of excessive cortisol secretion according to literature reported from different centres [8–10]. Based on the data reported herein, the cortisol AV: PV ratio was far greater than 6.5, and the ratio changed dramatically over time in patients without excessive cortisol secretion. Furthermore, the cortisol ratio between the high and low sides was greater than 2 in half of the AVS patients with normal cortisol secretion. Therefore, two factors might interfere with the validity of AVS in adrenal-dependent CS with bilateral adrenal masses: (1) the variation of cortisol in AVS induced by stress or fluctuation of ACTH and (2) the different dilutional effect in the right and left adrenals due to AV anatomy.

To exclude the possibility of endogenous ACTH secretion interfering with the interpretation of autonomous cortisol secretion, all patients underwent AVS while receiving dexamethasone in Young's study [18]. However, not all of the studies followed this protocol, and the utility of the DST has been questioned [7, 8, 10]. It is well known that ACTH is fully suppressed in the majority of patients with ACTH-independent CS. However, it is possible that minor ACTH-independent cortisol secretion occurs from all adrenal glands, even in the setting of suppressed ACTH secretion [8]. Furthermore, dexamethasone suppression cannot eliminate the dilutional difference between the right and left adrenal veins.

The most reliable solution is to investigate novel analytes to correct for cortisol lateralization during AVS. In PA patients, "cortisol-corrected" aldosterone ratios are compared to determine whether a unilateral source of aldosterone exists. Previous studies attempted to use epinephrine or aldosterone to correct for the side-to-side cortisol gradient [7–9]. Based on the data of Freel EM et al., in patients without pheochromocytoma, a gradient in catecholamine production between the right and left adrenal glands can be a normal finding. In the case, up to 83-fold difference in epinephrine was found between the right and left adrenal veins [11]. As a result, catecholamines are of no value in correcting the cortisol gradient. Aldosterone and cortisol are both adrenal cortical hormones. However, compared to cortisol, the secretion of aldosterone is mildly regulated by ACTH. Therefore, it is predictable that the use of aldosterone might correct for the cortisol lateralization ratio caused by the dilutional effect but not by stress or fluctuation of ACTH. Thus, it is not surprising that the diagnosis by AVS in two cases proved to be incorrect in patients with bilateral adrenal masses and ACTH-independent CS [8, 9].

The adrenal androgens androstenedione and DHEA are adrenocortical products. Compared to cortisol, higher gradients of AV to PV plasma androstenedione and DHEA concentrations were detected [15, 19]. Most importantly,

cortisol and adrenal androgens are both regulated by ACTH [20, 21]. As demonstrated in our study, androstenedione and DHEA closely correlated with cortisol. These merits make adrenal androgens ideal analytes to correct for cortisol variation or side-to-side dilutional differences in adrenal veins during AVS. In patients with normal cortisol secretion, the cortisol lateralization ratio caused by variation or dilutional differences almost disappeared after correction with androstenedione and DHEA.

5. Additional Points

Study Limitations. There are several limitations of the present study as follows. (1) The present study did not investigate the effectiveness of the DST on cortisol variation in patients without excessive cortisol secretion. It is suspected that the DST will alleviate the variation in cortisol levels in AVS induced by stress or the fluctuation in ACTH to some extent, but it has no effect on the different dilutions in the right and left adrenals due to AV anatomy. (2) The present data were obtained from patients with PA and normal cortisol secretion, and we did not provide evidence for the use of androstenedione and DHEA to correct AVS in patients with ACTH-independent CS. We recently showed the effectiveness of adrenal androgens in one case in clinical practice. Additional cases are needed to confirm the effectiveness of androstenedione and DHEA to correct for cortisol lateralization in ACTH-independent CS.

In conclusion, the present study promoted the use of the plasma adrenal androgens as normalizers to assess cortisol lateralization in AVS. This technique will improve the diagnostic accuracy of AVS in the localization of autonomous hypercortisolism in the setting of ACTH-independent CS in patients with bilateral adrenal masses.

Data Availability

The data used to support the findings of this study are included within the article.

Conflicts of Interest

The authors declare no conflicts of interest.

Authors' Contributions

(1) Ping Li and Dalong Zhu formed subject design. (2) Wenjing Zhang, Keying Zhu, Hongyun Li, and Yan Zhang were responsible for collecting and collating data. (3) Xuebin Zhang was responsible for adrenal venous sampling in DSA. (4) Wenjing Zhang and Keying Zhu performed data analysis. (5) Ping Li and Dalong Zhu performed result analysis. (6) Wenjing Zhang and Keying Zhu wrote the paper. Wenjing Zhang and Keying Zhu contributed equally to this paper.

Acknowledgments

This work was supported by the Natural Science Foundation of Jiangsu Province (Grant number BK20181116) and the Project of Jiangsu Provincial Medical Youth Talent.

References

[1] A. H. Maghrabi, A. Yaqub, K. L. Denning, N. Benhamed, S. Faiz, and T. Saleem, "Challenges in the diagnostic work-up and management of patients with subclinical cushing's syndrome and bilateral adrenal masses," *Endocrine Practice*, vol. 19, no. 3, pp. 515–521, 2013.

[2] L. K. Nieman, B. M. Biller, J. W. Findling et al., "Treatment of Cushing's syndrome: an endocrine society clinical practice guideline," *The Journal of Clinical Endocrinology & Metabolism*, vol. 100, no. 8, pp. 2807–2831, 2015.

[3] J. W. Funder, R. M. Carey, F. Mantero et al., "The management of primary aldosteronism: case detection, diagnosis, and treatment: an endocrine society clinical practice guideline," *The Journal of Clinical Endocrinology & Metabolism*, vol. 101, no. 5, pp. 1889–1916, 2016.

[4] G. P. Rossi, R. J. Auchus, M. Brown et al., "An expert consensus statement on use of adrenal vein sampling for the subtyping of primary aldosteronism," *Hypertension*, vol. 63, no. 1, pp. 151–160, 2014.

[5] E. J. Ku, A. R. Hong, Y. A. Kim, J. H. Bae, M. S. Chang, and S. W. Kim, "Adrenocorticotropic hormone-independent cushing syndrome with bilateral cortisol-secreting adenomas," *Endocrinology and Metabolism Clinics of North America*, vol. 28, no. 2, pp. 133–137, 2013.

[6] Y. W. Guo, C. M. Hwu, J. G. Won et al., "A case of adrenal Cushings syndrome with bilateral adrenal masses," in *Endocrinology Diabetes & Metabolis case Reports*, vol. 2016, 1, 1 edition, 2016.

[7] J. Wei, S. Li, Q. Liu et al., "ACTH-independent Cushing's syndrome with bilateral cortisol-secreting adrenal adenomas: a case report and review of literatures," *BMC Endocrine Disorders*, vol. 18, no. 1, pp. 22–29, 2018.

[8] R. G. Martins, R. Agrawal, D. M. Berney et al., "Differential diagnosis of adrenocorticotropic hormone-independent cushing syndrome: role of adrenal venous sampling," *Endocrine Practice*, vol. 18, no. 6, pp. e153–e157, 2012.

[9] C. E. Builes-Montaño, C. A. Villa-Franco, A. Román-Gonzalez, A. Velez-Hoyos, and S. Echeverri-Isaza, "Adrenal venous sampling in a patient with adrenal Cushing syndrome," *Colombia Médica*, vol. 46, no. 2, pp. 84–87, 2015.

[10] K. Cheng, W. Zhou, B. Huang et al., "Diagnosis and treatment of Cushing's syndrome caused by bilateral solitary adrenal neoplasma," *The Journal of Clinical Endocrinology and Metabolism*, vol. 32, no. 6, pp. 494–498, 2016.

[11] E. M. Freel, A. W. Stanson, G. B. Thompson et al., "Adrenal venous sampling for catecholamines: a normal value study," *The Journal of Clinical Endocrinology and Metabolism*, vol. 95, no. 3, pp. 1328–1332, 2010.

[12] T. M. Seccia, D. Miotto, M. Battistel et al., "A stress reaction affects assessment of selectivity of adrenal venous sampling and of lateralization of aldosterone excess in primary aldosteronism," *European Journal of Endocrinology*, vol. 166, no. 5, pp. 869–875, 2012.

[13] M. Tanemoto, T. Suzuki, M. Abe, T. Abe, and S. Ito, "Physiologic variance of corticotropin affects diagnosis in adrenal vein

sampling," *European Journal of Endocrinology*, vol. 160, no. 3, pp. 459–463, 2009.

[14] G. Ceolotto, G. Antonelli, G. Maiolino et al., "Androstenedione and 17-α-hydroxyprogesterone are better indicators of adrenal vein sampling selectivity than cortisol," *Hypertension*, vol. 70, no. 2, pp. 342–346, 2017.

[15] H. Li, X. Zhang, S. Shen et al., "Adrenal androgen measurement for assessing the selectivity of adrenal venous sampling in primary aldosteronism," *Steroids*, vol. 134, pp. 16–21, 2018.

[16] G. Eisenhofer, T. Dekkers, M. Peitzsch et al., "Mass spectrometry-based adrenal and peripheral venous steroid profiling for subtyping primary aldosteronism," *Clinical Chemistry*, vol. 62, no. 3, pp. 514–524, 2016.

[17] J. W. Funder, R. M. Carey, C. Fardella et al., "Case detection, diagnosis, and treatment of patients with primary aldosteronism: an endocrine society clinical practice guideline," *The Journal of Clinical Endocrinology & Metabolism*, vol. 93, no. 9, pp. 3266–3281, 2008.

[18] W. F. Young, H. du Plessis, G. B. Thompson et al., "The clinical conundrum of corticotropin-independent autonomous cortisol secretion in patients with bilateral adrenal masses," *World Journal of Surgery*, vol. 32, no. 5, pp. 856–862, 2008.

[19] M. Peitzsch, T. Dekkers, M. Haase et al., "An LC–MS/MS method for steroid profiling during adrenal venous sampling for investigation of primary aldosteronism," *The Journal of Steroid Biochemistry and Molecular Biology*, vol. 145, pp. 75–84, 2015.

[20] D. C. Aron, J. W. Fingdling, and J. B. Tyrrell, *Basic & Clinical Endocrinology*, McGraw-Hill, New York, NY, USA, 6th edition, 2001.

[21] A. Turcu, J. M. Smith, R. Auchus, and W. E. Rainey, "Adrenal androgens and androgen precursors-definition, synthesis, regulation and physiologic actions," *Comprehensive Physiology*, vol. 4, no. 4, pp. 1369–1381, 2014.

Hindawi
International Journal of Endocrinology
Volume 2019, Article ID 4828402, 7 pages
https://doi.org/10.1155/2019/4828402

Research Article

The Association between a 24-Hour Blood Pressure Pattern and Circadian Change in Plasma Aldosterone Concentration for Patients with Aldosterone-Producing Adenoma

Hai Li,[1] Jianbin Liu,[2,3] Juan Liu,[1] Liehua Liu,[1] Minmin Huang,[1] Guohong Wei,[1] Wanping Deng,[1] Zhimin Huang,[1] Xiaopei Cao,[1] Haipeng Xiao,[1] and Yanbing Li[1]

[1]*Department of Endocrinology and Diabetes Center, The First Affiliated Hospital of Sun Yat-sen University, Guangzhou, Guangdong 510080, China*
[2]*Department of Medicine, Eastern Health, Box Hill, VIC 3128, Australia*
[3]*Centre for Eye Research Australia, University of Melbourne, Parkville, VIC 3001, Australia*

Correspondence should be addressed to Yanbing Li; easd04lyb@126.com

Received 27 November 2018; Revised 14 April 2019; Accepted 6 May 2019; Published 29 July 2019

Guest Editor: Rosa M. Paragliola

The absence of nocturnal blood pressure (BP) decline is associated with hypertensive complications. Data regarding circadian BP patterns in patients with aldosterone-producing adenoma (APA) are limited and equivocal. We evaluated the circadian BP profile in patients with APA and its relationship with the circadian aldosterone rhythm. BP in patients with APA and in those with essential hypertension (EH) were assessed through in-hospital 24-h ambulatory blood pressure monitoring. Over a 24-h in-hospital period, plasma aldosterone levels taken at midnight, 0400, 0800, 1200, 1600, and 2000 h were measured. To evaluate a correlation between BP and hormone rhythm, we included 27 patients with APA (APA group) and 27 patients with EH (EH group). Both groups had similar age, sex ratio, body mass index, duration of hypertension, family history of hypertension, and lipid profiles. The day-night BP differences in both patient groups were similar, whether expressed as absolute values or percentages. The proportions of patients with dipping BP profiles were also comparable (APA group, 5 of 27; EH group, 7 of 27; $\chi 2 = 0.429$; $P = 0.513$). At each time point, APA group plasma aldosterone concentrations (PACs) were higher than those of the EH group. A circadian change in relation to PAC was observed in both groups. A correlation between PAC and BP was statistically nonsignificant in most study patients in either group. Our data indicated that the circadian BP pattern was not associated with a change in PAC levels in patients with APA.

1. Introduction

Observational studies have shown a 10%–20% decline in blood pressure (BP) levels during sleep at night in most normotensive individuals and in patients with essential hypertension [1, 2]. The term "dipper" refers to individuals with normal nocturnal fall of blood pressure (BP) and "nondipper" refers to those whose BP does not fall nocturnally. A nondipping BP pattern is associated with hypertensive complications [3].

Data regarding circadian BP patterns in patients with aldosterone-producing adenoma (APA) are limited and equivocal. Previous studies have reported that a circadian BP decline was blunted in APA patients [4, 5], which might contribute to increased cardiovascular disease risk in this population.

It is generally known that, in aldosteronism, overproduction of aldosterone leads to increased sodium and water retention and subsequent hypertension via its genomic effect, which is a relatively long-term action. Recent studies [6] have revealed rapid effects of aldosterone on vascular tone; thus, raising the possibility that aldosterone might play a role in short-term BP regulation.

For patients with APA, it remains unclear whether an increase of plasma aldosterone concentration (PAC) or its change might affect the circadian BP pattern. This study aimed to evaluate the circadian BP profile in patients with APA and its relationship with PAC.

2. Methods and Materials

2.1. Patients. The study participants comprised patients who had been consecutively referred to our center from June 2011 to March 2013 because of suspected primary aldosteronism (PA) or to exclude secondary hypertension (refractory hypertension [uncontrolled hypertension despite the use of at least 5 different classes of antihypertensive agents], spontaneous or drug-induced hypokalemia, onset in youth [<40 years old], or adrenal incidentaloma). The protocol and informed consent documents were approved by the research ethics board of Sun Yat-sen University. All patients provided their written informed consent.

2.2. Preparation of Assessments. Before and during the biochemical evaluation, phenoxybenzamine was administered to control BP, if necessary. Spironolactone or amiloride was discontinued at least 6 weeks prior to evaluation, as were angiotensin receptor blockers, angiotensin converting enzyme inhibitors, or thiazide diuretics at least 4 weeks prior to evaluation. Daily natrium and potassium supplements (160 mEq and 60 mEq, respectively) were administered during the assessment period.

2.3. Diagnosis of Primary Aldosterone and Aldosterone-Producing Adenoma. We followed study methods previously described by Yanbing Li et al. in 2017 [7], and all patients underwent a standard diagnostic procedure including repeated measurements of serum potassium, and 24-h urinary aldosterone, plasma aldosterone, and renin activity. For those with elevated urinary aldosterone levels, elevated serum aldosterone levels, or elevated aldosterone-renin ratios, upright-furosemide loading tests [8] were performed as confirmatory tests. A diagnosis of PA was confirmed if plasma renin activity (PRA) levels were <2 ng/ml/h after challenge.

An adrenal spiral computed tomography scan with sections at 0.3 mm intervals was conducted. Once an adrenal lesion was located, adrenalectomy was recommended. The final diagnosis of APA was later confirmed with pathology tests plus correction of hypokalemia postoperatively.

2.4. Ambulatory Blood Pressure Monitoring and Simultaneous/Synchronous Hormone Assessment. All in-patients received continuous noninvasive 24-h ambulatory blood pressure monitoring (ABPM) (TM 2430, Higashi-Ikebukuro, Toshima-ku, Tokyo) during hospitalization, following the same standard operating procedures as ambulatory blood pressure monitoring for out-patients. The monitor recorded systolic and diastolic BP every 30 min during the daytime (0700 to 2300 h) and every 60 min through the night (2300 to 0700 h). The ambulatory data were included in the analysis if the monitoring period was >20 h and there were no periods of >2 h without measurements. Dippers or a dipping BP pattern were defined as >10% decline in both systolic and diastolic BP [9, 10].

Within 24 hours of in-patient ABPM, blood samples were drawn at midnight, 0400, 0800, 1200, 1600, and 2000 h, for measurements of plasma aldosterone.

2.5. Exclusion of Secondary Hypertension due to Other Common Causes. Urine tests, measurements of serum creatinine, 24-h urine free cortisol, 24-h urine vanillylmandelic acid, and ultrasonography of renal arteries and veins were performed to screen common secondary causes of hypertension. Patients with renal hypertension, pheochromocytoma, or Cushing's syndrome were excluded. If the above tests including 24-h urinary aldosterone, plasma aldosterone, renin activity and aldosterone-renin ratios, 24-h urine free cortisol, 24-h urine vanillylmandelic acid, 24-h urine free cortisol, and 24-hour urine vanillylmandelic acid were normal, a diagnosis of nonfunctional adrenal tumor would be made.

2.6. Statistical Analysis. All statistical analyses were performed using SPSS 13.0. Values are expressed as mean ± SD, unless otherwise noted. Values between groups were compared using a two-tailed t-test. Variables that were not normally distributed were log transformed before analyses. Categorical values were compared using a chi-squared test. The correlation between PAC and BP was evaluated using a Pearson's test for each patient. Logistic analysis was performed to evaluate the independent predictors of dipping BP patterns in both groups. Statistical significance was considered at a value of $P < 0.05$.

3. Results

3.1. Demographic, Clinical, and Biochemical Profiles of the Study Participants. Forty patients were recruited, of whom 13 were excluded for other causes of secondary hypertension. Twenty-seven patients with APA (APA group) were included and received biochemical and in-patient ABPM assessments, as did 27 patients with EH (EH group). No participants received any antihypertensive medication during the evaluation.

Demographic, biochemical, and hormone values of the two groups are shown in Table 1. The two groups had similar age, sex ratio, body mass index, duration of hypertension, family history of hypertension, and lipid profiles. The patients with APA had lower serum potassium concentration and plasma renin activity, and higher PAC, aldosterone-renin ratio, and 24-h aldosterone secretion, compared to patients with EH.

3.2. Blood Pressure Measurements. BP profiles of the two groups are presented in Table 2. The day-night BP differences in patients with APA were similar to those in patients with EH, whether expressed as an absolute value or a percentage. Proportions of patients with dipping BP were also comparable between the two groups (APA group, 5 of 27 patients vs. EH group, 7 of 27; $\chi^2 = 0.429$; $P = 0.513$).

3.3. Circadian Change of Plasma Aldosterone Concentration. The circadian profiles of PAC in the two groups of patients are shown in Figure 1. The two groups had a similar trend over 24 h, with a peak at 0800 h and a nadir at midnight in each group; however, the EH group had much lower levels at

Table 1: Demographic and biochemical values in patients with aldosterone-producing adenoma and essential hypertension.

	APA (n = 27)	EH (n = 27)	P-value
Age (years)	45.9 ± 11.0	41.6 ± 12.4	0.188
Sex (male/female)	13/14	13/14	1.000
Body mass index (kg/m^2)	23.7 ± 3.7	24.5 ± 3.6	0.407
Duration of hypertension (weeks)*	153 (58, 330)	156 (46,306)	0.945
Family history of hypertension (yes/no)	15/12	14/13	1.000
Serum potassium (mmol/L)	2.62 ± 0.71	3.62 ± 0.55	<0.001
Serum total cholesterol (mmol/L)	4.64 ± 1.09	4.88 ± 1.12	0.450
Serum triglyceride (mmol/L)	1.25 ± 0.57	1.43 ± 1.32	0.518
Serum HDL-c (mmol/L)	1.24 ± 0.29	1.15 ± 0.25	0.200
Serum LDL-c (mmol/L)	3.02 ± 0.97	3.27 ± 0.99	0.368
Basal PAC (ng/dL)	21.8 ± 6.3	18.1 ± 6.5	0.049
Post challenge PAC (ng/dL)	23.5 ± 7.2	18.5 ± 4.6	0.006
Basal PRA (ng/mL/h)*	0.050 (0.040, 0.308)	1.665 (1.052, 3.247)	<0.001
Post challenge PRA (ng/mL/h)*	0.058 (0.052, 0.326)	6.887 (4.587, 10.86)	<0.001
Basal ARR*	306 (240, 574)	12.9 (8.7, 35.9)	<0.001
Post challenge ARR*	339 (219, 670)	2.89 (1.64, 6.75)	<0.001
24-h urine aldosterone (ug/24-hour)	4.92 ± 2.69	3.1 1 ± 1.84	0.019

*not normally distributed, data expressed as median (25th percentile, 75th percentile)
APA, aldosterone-producing adenoma; EH, essential hypertension; PAC, plasma aldosterone concentration; PRA, plasma renin activity; ARR, aldosterone renin ratio, calculated as PAC (ng/dL)/PRA (ng/mL/h)

Table 2: Comparison of blood pressure measurements between patients with aldosterone-producing adenoma and essential hypertension.

	APA (n = 27)	EH (n = 27)	P value
Mean BP (mm Hg)			
day time SBP	143.8 ± 13.3	137.9 ± 18.5	0.188
day time DBP	94.2 ± 10.4	89.4 ± 15.5	0.189
night time SBP	137.8 ± 15.0	130.3 ± 19.6	0.120
night time DBP	87.9 ± 11.9	83.0 ± 17.7	0.242
Day-night BP difference (mm Hg)			
SBP	5.85 ± 9.40	7.63 ± 11.20	0.530
DBP	6.41 ± 6.34	6.30 ± 6.78	0.951
Relative night time decline (%)			
SBP	4.01 ± 6.52	5.38 ± 7.85	0.490
DBP	6.84 ± 6.91	7.24 ± 8.21	0.845
BP pattern (dipper/nondipper)*	5/22	7/20	0.513

*dippers were defined as those with a >10% decline in both systolic and diastolic blood pressure
Note: day-night BP difference calculated as day time BP minus night time BP, and relative night time decline calculated as: (day time BP − night time BP) ÷ day time BP × 100%
APA, aldosterone-producing adenoma; BP, blood pressure; DBP, diastolic blood pressure; EH, essential hypertension; SBP, systolic blood pressure

night. The PAC of the APA patients at each time point was higher than that of the EH patients.

3.4. Circadian Variation of Blood Pressure and Plasma Aldosterone Concentration. The circadian change of BP and concomitant PAC in each group are shown in Figure 2. Considering that aldosterone might have a delayed effect on vascular tone (6), we performed linear correlation of PAC with BP recorded at two time points: (1) the time of blood sampling for aldosterone measurement and (2) 1 h after blood sampling. No statistical significance was found (Table 3).

3.5. Pearson's Correlation of Plasma Aldosterone Concentration and Blood Pressure. To ensure a more precise and detailed evaluation, a Pearson's correlation of BP and PAC was conducted for each patient, and the results are presented in Figure 3. The correlation was nonsignificant in most of the studied patients. Logistic regression did not find any independent predictor for dipper BP profiles in either group.

4. Discussion

In the present study, we did not find any significant differences in BP level, nocturnal BP decline, or the proportion

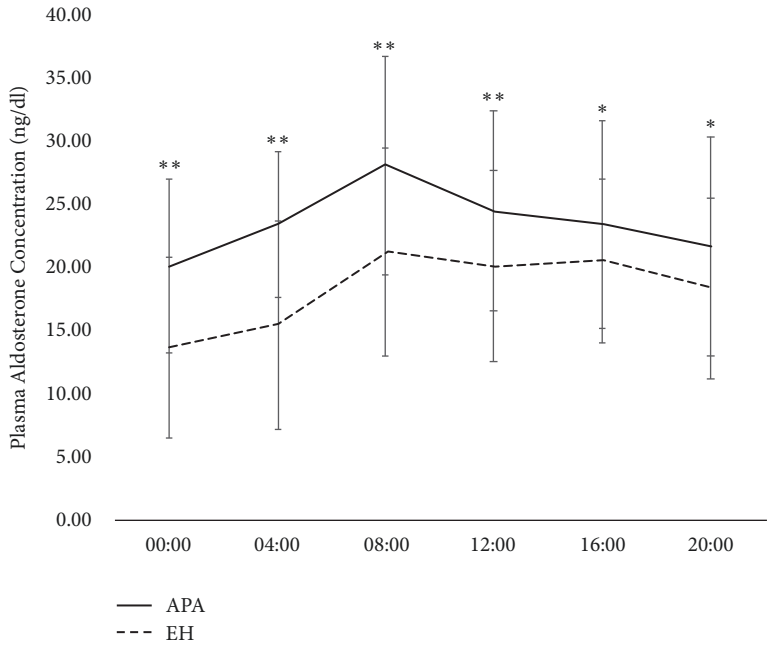

	00:00	04:00	08:00	12:00	16:00	20:00
APA (ng/dl)	20.2±6.9∗∗	23.5±5.8∗∗	28.2±8.7∗∗	24.5±7.9∗∗	23.5±8.3∗	21.7±8.7∗
EH (ng/dl)	13.7±7.2	15.5±8.3	21.3±8.3	20.2±7.6	20.6±6.5	18.4±7.2

Figure 1: *The circadian change in relation to plasma aldosterone concentration* vs. that in the EH group. $*P < 0.05$; $**P < 0.01$. Note: the solid line refers to patients with APA, while the dashed line refers to patients with EH. APA, aldosterone-producing adenoma; EH, essential hypertension.

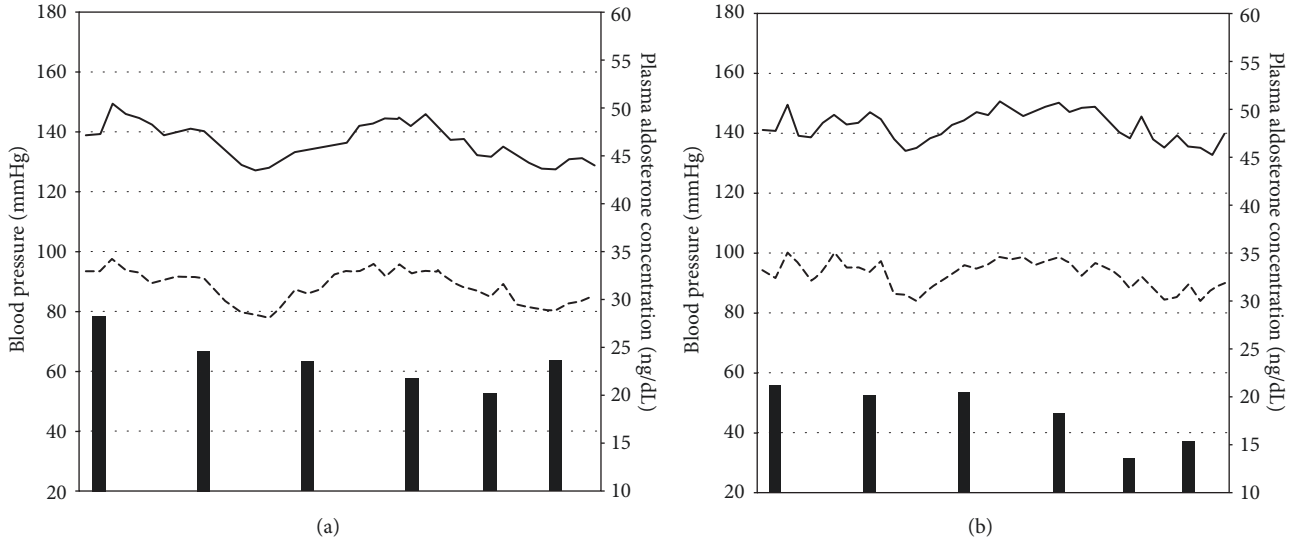

Figure 2: *Circadian variation of blood pressure and plasma aldosterone concentration in patients with aldosterone-producing adenoma (a) and patients with essential hypertension (b).* Note: the solid line represents systolic blood pressure, the dashed line represented diastolic blood pressure, and the bars represent plasma aldosterone concentration.

of patients with a dipping BP pattern, between patients with APA and those with EH, which is consistent with some previous reports [4, 5, 11–15]. However, other studies have shown differing results. Rabbia et al. found significantly fewer dippers among patients with APA in comparison to patients with EH [16]. Less amplitude in the nocturnal fall of BP was also observed in patients with APA [16, 17]. Of note, in the abovementioned studies and in the present study, the absolute proportion of dippers among patients with APA varied significantly, from 18.5% to 91.7%. Thus,

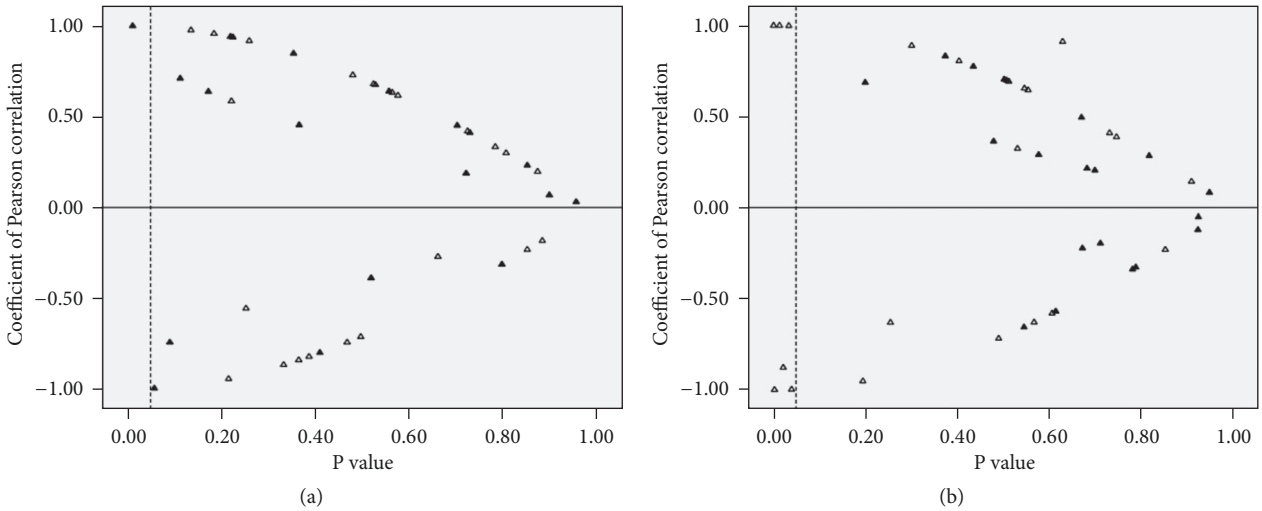

Figure 3: *Pearson correlation of plasma aldosterone concentration and blood pressure ((a) systolic, (b) diastolic) for each patient*. The x-axis represents the P-value yielded according to Pearson's correlations. The dotted line indicates P = 0.05. Most P-values were higher than 0.05 (distributed to the right of the dotted line). Note: each triangle represents a specific patient. A hollow triangle represents a patient with EH and a solid triangle represents a patient with APA.

Table 3: Linear correlation of plasma aldosterone concentration and blood pressure.

	APA				EH			
	SBP*	SBP1h**	DBP*	DBP1h**	SBP*	SBP1h**	DBP*	DBP1h**
R	0.306	0.471	0.446	0.390	0.559	0.539	0.611	0.742
P	0.556	0.345	0.375	0.444	0.248	0.270	0.198	0.091

*BP recorded at the time of blood sampling for aldosterone measurement
**BP recorded 1 h after blood sampling for aldosterone measurement
APA, patients with aldosterone-producing adenoma; BP, blood pressure; DBP, diastolic blood pressure; EH, patients with essential hypertension; SBP, systolic blood pressure

based on current data, we cannot yet draw any unequivocal conclusions concerning the BP pattern in patients with APA. When comparing these results, factors such as sample size, medication, daily activity, and sodium intake should be considered.

Previous studies have shown that, in APA patients, the circadian aldosterone change was similar to that of normotensive individuals and those with EH [18–21]. Similarly, in the present study, the diurnal rhythm of plasma aldosterone was present in both APA and EH patients, with a peak at 0800 h and a nadir at midnight (Figure 1). Pathologic production of aldosterone due to APA seemed only to increase PAC but did not modify its circadian rhythm.

The main finding in our study was the absence of statistically significant correlations between PAC and concomitant SBP and DBP (Table 3; Figure 3) in either patients with APA or patients with EH. Furthermore, to assess a delayed effect, linear correlation between aldosterone and BP values was recorded 1 h after the blood sample collection was also performed and still yielded nonsignificant results (Table 3). Therefore, it is likely that aldosterone imposed a minimal instant/short-term (hourly) effect on BP regulation, or that such effect, if any, was so weak that it could be easily confounded due to other mechanisms. Of note, findings from previous studies have been inconsistent. Using a relatively small sample (n = 5), Nicholls et al. [21] reported there was no significant relationship between the plasma aldosterone level and concomitant arterial BP in patients with PA. Imai et al. [11] speculated that aldosterone mediated the BP rhythm, based on their finding that the circadian rhythm of BP and PAC appeared to be synchronous.

A rapid direct vascular effect of aldosterone has recently been reported [6]. In an in vivo study on human forearm vascular reactivity, Romagni et al. [22] reported a rapid vasoconstrictive effect of aldosterone at physiological concentrations. Gunaruwan et al. [23] reported that aldosterone had no acute effect on forearm resistance vessels in healthy male volunteers, which was clearly different from results reported by Romagni et al. and Schmidt et al., who also in turn demonstrated contrary effects of aldosterone on the vascular wall [24, 25]. These inconsistent in vivo study results appear to raise more questions concerning how aldosterone acts on BP regulation than they have attempted to answer.

Some possible mechanisms through which secondary hypertension may modify the circadian BP include sympathetic nervous system activation, fluid retention, and increases in peripheral vascular resistance. Inappropriate activation of the sympathetic nervous system during sleep has

been considered to be a major factor contributing to elevation of sleep BP in pheochromocytoma [26], hyperthyroidism [26], and sleep apnea [27]. However, this is not the case in primary aldosteronism [28]. Uzu et al. indicated that sodium restriction shifted the circadian BP rhythm from "nondipper" to "dipper" status in salt-sensitive patients with EH [29] and restored the nocturnal BP dip in those with APA [30].

Our study had some limitations. The sample size was relatively small. Within the 24-h in-hospital ABPM, blood samples for measurements of plasma aldosterone were drawn at midnight, 0400, 0800, 1200, 1600, and 2000 h; and blood sampling and hospitalization may have impaired sleeping patterns and the nocturnal dip of BP. This could have had a significant effect on the results. Moreover, we only measured seven time points for plasma aldosterone, and it is possible that more frequent blood sampling for aldosterone measurement would have offered a more precise estimation of the aldosterone rhythm. We used 24-h urine vanillylmandelic acid to exclude pheochromocytoma; however, this is not the gold standard method for the diagnosis of pheochromocytoma. These major limitations are likely to have weakened the strength of our research and should be taken into consideration when analyzing or applying the findings of our study.

Studies with larger samples and with more frequent blood sampling for aldosterone measurement or studies that use another technique that is not affected due to hospitalization are warranted to further evaluate the circadian BP profile in patients with APA and its relationship with circadian aldosterone rhythm.

In conclusion, the circadian BP pattern was not associated with a change in PAC in patients with APA. Further studies are needed to address the mechanisms involved in the reduction of nocturnal BP decline in patients with APA.

Abbreviations

APA: Aldosterone-producing adenoma
BP: Blood pressure
DBP: Diastolic blood pressure
EH: Essential hypertension
PA: Primary aldosteronism
PAC: Plasma aldosterone concentration
PRA: Plasma renin activity
SBP: Systolic blood pressure.

Data Availability

The data used to support the findings of this study are available from the corresponding author upon request.

Conflicts of Interest

The authors declare no conflicts of interest.

Authors' Contributions

Hai Li and Jianbin Liu contribute equally to this work.

Acknowledgments

We would like to thank all the doctors, nurses, technicians, and patients involved for their dedication to the study. This research was supported by grants from the National Natural Science Foundation of China (nos. 81572623, 81572624, and 81602347) and the Natural Science Foundation of Guangdong Province (no. 2016A030310169).

References

[1] M. W. Millar-Craig, C. N. Bishop, and E. B. Raftery, "Circadian variation of blood pressure," *The Lancet*, vol. 311, no. 8068, pp. 795–797, 1978.

[2] J. A. Staessen, R. H. Fagard, P. J. Lijnen, L. Thijs, R. Van Hoof, and A. K. Amery, "Mean and range of the ambulatory pressure in normotensive subjects from a meta-analysis of 23 studies," *American Journal of Cardiology*, vol. 67, no. 8, pp. 723–727, 1991.

[3] T. G. Pickering, "The clinical significance of diurnal blood pressure variations. Dippers and nondippers," *Circulation*, vol. 81, no. 2, pp. 700–702, 1990.

[4] T. Zelinka and J. Widimský, "Twenty-four hour blood pressure profile in subjects with different subtypes of primary aldosteronism," *Physiological Research*, vol. 50, no. 1, pp. 51–57, 2001.

[5] G. A. Mansoor and W. B. White, "Circadian blood pressure variation in hypertensive patients with primary hyperaldosteronism," *Hypertension*, vol. 31, no. 3, pp. 843–847, 1998.

[6] J. W. Funder, "The nongenomic actions of aldosterone," *Endocrine Reviews*, vol. 26, no. 3, pp. 313–321, 2005.

[7] H. Li, J. Liu, X. Feng et al., "Favorable surgical outcomes of aldosterone-producing adenoma based on lateralization by CT imaging and hypokalemia: a non-AVS-based strategy," *International Urology and Nephrology*, vol. 49, no. 12, pp. 2151–2156, 2017.

[8] T. Nishikawa, M. Omura, F. Satoh et al., "Guidelines for the diagnosis and treatment of primary aldosteronism -The Japan Endocrine Society 2009-," *Endocrine Journal*, vol. 58, no. 9, pp. 711–721, 2011.

[9] P. Verdecchia, C. Porcellati, G. Schillaci et al., "Ambulatory blood pressure: An independent predictor of prognosis in essential hypertension," *Hypertension*, vol. 24, no. 6, pp. 793–801, 1994.

[10] A. V. Chobanian, G. L. Bakris, H. R. Black et al., "Seventh report of the Joint National Committee on prevention, detection, evaluation, and treatment of high blood pressure," *Hypertension*, vol. 42, no. 6, pp. 1206–1252, 2003.

[11] Y. Imai, K. Abe, S. Sasaki et al., "Altered circadian blood pressure rhythm in patients with Cushing's syndrome," *Hypertension*, vol. 12, no. 1, pp. 11–19, 1988.

[12] M. Penzo, P. Palatini, G. P. Rossi, L. Zanin, and A. C. Pessina, "In primary aldosteronism the circadian blood pressure rhythm is similar to that in primary hypertension," *Clinical and Experimental Hypertension*, vol. 16, no. 5, pp. 659–673, 2009.

[13] S. Zacharieva, M. Orbetzova, A. Elenkova et al., "Diurnal blood pressure pattern in patients with primary aldosteronism," *Journal of Endocrinological Investigation*, vol. 29, no. 1, pp. 26–31, 2006.

[14] Y. Kimura, M. Kawamura, S. Onodera, and K. Hiramori, "Controlled study of circadian rhythm of blood pressure in patients with aldosterone-producing adenoma compared with

those with essential hypertension," *Journal of Hypertension*, vol. 18, no. 1, pp. 21–25, 2000.

[15] M. Ceruti, L. Petramala, D. Cotesta et al., "Ambulatory blood pressure monitoring in secondary arterial hypertension due to adrenal diseases," *The Journal of Clinical Hypertension*, vol. 8, no. 9, pp. 642–648, 2006.

[16] F. Rabbia, F. Veglio, G. Martini et al., "Fourier analysis of circadian blood pressure profile in secondary hypertension," *Journal of Human Hypertension*, vol. 11, no. 5, pp. 295–299, 1997.

[17] Y. Imai, K. Abe, S. Sasaki et al., "Circadian blood pressure variation in patients with renovascular hypertension or primary aldosteronisn," *Clinical and Experimental Hypertension. Part A: Theory and Practice*, vol. 14, no. 6, pp. 1141–1167, 2009.

[18] F. H. Katz, P. Romfh, J. A. Smith, E. F. Roper, J. S. Barnes, and J. B. Boyd, "Diurnal variation of plasma aldosterone, cortisol and renin activity in supine man," *The Journal of Clinical Endocrinology & Metabolism*, vol. 40, no. 1, pp. 125–134, 1975.

[19] M. Schambelan, N. L. Brust, B. C. Chang, K. L. Slater, and E. G. Biglieri, "Circadian rhythm and effect of posture on plasma aldosterone concentration in primary aldosteronism," *The Journal of Clinical Endocrinology & Metabolism*, vol. 43, no. 1, pp. 115–131, 1976.

[20] J. P. Cain, M. L. Tuck, G. H. Williams, R. G. Dluhy, and S. H. Rosenoff, "The regulation of aldosterone secretion in primary aldosteronism," *American Journal of Medicine*, vol. 53, no. 5, pp. 627–637, 1972.

[21] M. G. Nicholls, E. A. Espiner, H. Ikram, A. H. Maslowski, E. J. Hamilton, and P. J. Bones, "Hormone and blood pressure relationships in primary aldosteronism," *Clinical and Experimental Hypertension. Part A: Theory and Practice*, vol. 6, no. 8, pp. 1441–1458, 2009.

[22] P. Romagni, F. Rossi, L. Guerrini, C. Quirini, and V. Santiemma, "Aldosterone induces contraction of the resistance arteries in man," *Atherosclerosis*, vol. 166, no. 2, pp. 345–349, 2003.

[23] P. Gunaruwan, M. Schmitt, J. Taylor, L. Lee, A. Struthers, and M. Frenneaux, "Lack of rapid aldosterone effects on forearm resistance vasculature in health," *Journal of the Renin-Angiotensin-Aldosterone System*, vol. 3, no. 2, pp. 123–125, 2016.

[24] B. M. Schmidt, A. Montealegre, C. P. Janson et al., "Short term cardiovascular effects of aldosterone in healthy male volunteers," *The Journal of Clinical Endocrinology & Metabolism*, vol. 84, no. 10, pp. 3528–3533, 1999.

[25] B. M. Schmidt, S. Oehmer, C. Delles et al., "Rapid nongenomic effects of aldosterone on human forearm vasculature," *Hypertension*, vol. 42, no. 2, pp. 156–160, 2003.

[26] S. Mann, D. G. Altman, E. B. Raftery, and R. Bannister, "Circadian variation of blood pressure in autonomic failure.," *Circulation*, vol. 68, no. 3, pp. 477–483, 1983.

[27] V. K. Somers, M. E. Dyken, M. P. Clary, and F. M. Abboud, "Sympathetic neural mechanisms in obstructive sleep apnea," *The Journal of Clinical Investigation*, vol. 96, no. 4, pp. 1897–1904, 1995.

[28] M. Munakata, Y. Imai, J. Hashimoto et al., "Normal sympathetic vasomotor and cardiac parasympathetic activities in patients with primary aldosteronism: assessment by spectral analysis," *Autonomic Neuroscience: Basic and Clinical*, vol. 52, no. 2-3, pp. 213–223, 1995.

[29] T. Uzu, K. Ishikawa, T. Fujii, S. Nakamura, T. Inenaga, and G. Kimura, "Sodium restriction shifts circadian rhythm of blood pressure from nondipper to dipper in essential hypertension," *Circulation*, vol. 96, no. 6, pp. 1859–1862, 1997.

[30] T. Uzu, M. Nishimura, T. Fujii et al., "Changes in the circadian rhythm of blood pressure in primary aldosteronism in response to dietary sodium restriction and adrenalectomy," *Journal of Hypertension*, vol. 16, no. 12, pp. 1745–1748, 1998.

Hindawi
International Journal of Endocrinology
Volume 2019, Article ID 7014240, 11 pages
https://doi.org/10.1155/2019/7014240

Research Article

Transcriptome Analysis Reveals Significant Differences in Gene Expression of Malignant Pheochromocytoma or Paraganglioma

Yong Joon Suh,[1] **Jung Ho Park**,[1] **Sanchir-Erdene Bilegsaikhan**,[1] **and Dong Jin Lee**[2]

[1]*Department of Breast and Endocrine Surgery, Hallym University Sacred Heart Hospital, Anyang 14068, Republic of Korea*
[2]*Department of Otolaryngology-Head and Neck Surgery, Hallym University College of Medicine, Seoul 07441, Republic of Korea*

Correspondence should be addressed to Yong Joon Suh; nicizm@gmail.com

Received 12 February 2019; Revised 13 April 2019; Accepted 18 April 2019; Published 8 May 2019

Guest Editor: Giampaolo Papi

Prediction of malignant behavior of pheochromocytoma (PC) or paraganglioma (PG) is of limited value. The Cancer Genome Atlas (TCGA) and the French 'Cortico et Médullosurrénale: les Tumeurs Endocrines' (COMETE) network in Paris (France) facilitate accurate differentiation of malignant PC/PG based on genetic information. Therefore, the objective of this transcriptome analysis is to identify the prognostic genes underlying the differentiation of malignant PC/PG in the TCGA and COMETE databases. TCGA carries data pertaining to multigenomic analysis of 173 PC/PG surgical resection samples while the COMETE cohort contains data involving 188 PC/PG surgical resection samples. Clinical information and mRNA expression datasets were downloaded from TCGA and COMETE databases. Based on eligibility criteria, 58 of 173 PC/PG samples in TCGA and 171 of 188 PC/PG samples collected by the COMETE network were selected. Using Ingenuity Pathway Analysis, the mRNA expression of malignant and benign PC/PG was compared. The 58 samples in TCGA included 11 malignant and 47 benign cases. Among the 171 samples obtained from the COMETE cohort, 19 were malignant and 152 were benign. A comparative analysis of the mRNA expression data of the two databases revealed that 11 up/downregulated pathways involved in malignant PC/PG were related to cancer signaling, metabolic alteration, and prominent mitosis, whereas 6 upregulated genes and 1 downregulated gene were significantly enriched in the functional annotation pathways. The TCGA and COMETE databases showed differences in mRNA expression associated with malignant and benign PC/PG. Improved recognition of prognostic genes facilitates the diagnosis and treatment of PC/PG.

1. Introduction

Pheochromocytoma (PC) is a catecholamine-secreting neuroendocrine neoplasm originating in the adrenal medulla [1]. Paraganglioma (PG) is a catecholamine-producing neuroendocrine neoplasm developing in the extra-adrenal chromaffin tissue of sympathetic ganglia. Nearly 15–20% of PC/PG originated in extra-adrenal chromaffin tissues whereas 80–85% of PC/PG develops from adrenal medulla. The annual incidence of PC/PG varies between 2 and 8 per million. In the population, the prevalence of PC/PG ranges from 1:6,500 to 1:2,500, respectively [2, 3]. Clinical manifestations include hypertension, tachycardia, headache, diaphoresis, and anxiety [4].

Diagnostic tests for PC/PG include imaging, biochemical evaluation, and histopathology, in addition to genetic testing [5–7]. Patients with PC/PG are managed via surgery, medical treatment, chemotherapy, targeted radiation therapy using ^{131}I-MIBG, embolization, cryoablation, targeted molecular therapy, and radiofrequency ablation [8]. Due to the diagnostic uncertainty, management usually entails vigilant monitoring for metastasis in PC/PG.

The tumor conforms to "the rule of 10s" and 10% of PC/PG is considered malignant [9, 10]. However, the malignancy rate exceeds 10% in patients with extra-adrenal disease [11]. Malignant PC/PG is associated with a 5-year survival rate of around 50% [12, 13]. The patients' long-term survival has yet to be improved [14].

Histological analysis cannot be used to predict the malignant or benign behavior of PC/PG [15]. According to the 8th edition of the American Joint Committee on Cancer (AJCC) staging system, distant metastasis is the only distinctive feature of malignant PC/PG. Therefore, this diagnostic limitation restricts therapeutic planning. Accurate diagnosis is directly linked to successful management. Institutions have struggled to define molecular markers for malignant PC/PG [16, 17]. Studies to discover robust predictors of malignancy are still ongoing [18, 19].

Recent molecular data obtained from The Cancer Genome Atlas (TCGA) and the French 'Cortico et Médullosurrénale: les Tumeurs Endocrines' (COMETE) cohort are available in the public domain [20–22]. The databases describe tumors including mRNA expression and clinical information. The TCGA and COMETE databases may be used for transcriptome analysis of malignant PC/PG. The aim of the present study was to identify potential biomarkers based on the mRNA expression profile of TCGA and COMETE databases for diagnosis of malignant PC/PG.

2. Materials and Methods

2.1. Study Design. Accessible data obtained from TCGA and COMETE cohort were used to compare malignant and benign PC/PG cases. The TCGA data contains multigenomic analysis of 173 PC/PG surgically resected samples. The initial pathological diagnosis was conducted from 1988 to 2013. Clinical information and gene expression dataset (20,531 genes) of RNA-sequencing mRNA Fragments Per Kilobase Million (FPKM) were downloaded from the TCGA database. The dataset was assembled into a table. Only samples with TCGA type code 01 (primary solid tumor) were included (Figure 1). Benign samples were included only if the follow-up exceeded two years. However, malignant samples were included even if they were metastasized within two years. Aggressive samples with local invasion or metastatic lymph nodes were excluded due to uncertain behavior. A total of 58 samples met the inclusion criteria. The 58 PC/PG samples included 11 malignant and 47 benign cases. Clinical characteristics and mRNA expression were reorganized according to tumor behavior and compared with each other. The COMETE cohort carried multiomic analytical data pertaining to 188 PC/PG surgically resected samples from the French COMETE Network. Cases were recruited from 1993 to 2008. Clinical information and expression dataset (39,534 probes) of mRNA transcripts were downloaded from the COMETE cohort. Only primary tumor samples were included (Figure 2). A total of 171 samples contained accessible genomic data and corresponding clinical information. The 171 samples included 19 malignant and 152 benign cases. Clinical characteristics and mRNA expression were reorganized according to behavior and compared. The gene expression was interpreted by extracting differentially expressed genes (DEGs) from TCGA and COMETE cohort. Commonly enriched genes were searched via Ingenuity Pathway Analysis (IPA). The identified genes were validated using the Dutch cohort (GSE67066) [23].

2.2. Definition. Metastasis was defined as the presence of chromaffin tissue at nonchromaffin sites distant from the primary tumor. Malignant or benign behavior was used to define metastasis or lack thereof, respectively. A zero value was filtered for the analysis of mRNA. To identify DEGs, a false discovery rate < 0.05 and a $\log_2$ fold change ≥ 1.5 were set as the threshold values. The functional enrichment of genes was analyzed based on Gene Ontology.

2.3. Statistics. Malignant and benign PC/PG groups were compared using Chi-squared test or Fisher's exact test for categorical data and Student's t-test or Mann-Whitney U test for continuous data without normal distribution. In two-tailed tests, a p value below 0.05 was considered statistical significant. Statistical analysis was performed using R 3.4.1 (R Foundation for Statistical Computing, Vienna, Austria), GSEA 2.1.0 (Broad Institute, MA, USA), and IPA (Ingenuity Systems, CA, USA). The overall survival rate was estimated according to the degree of gene expression using the UALCAN platform [24].

3. Results

3.1. Clinical Characteristics. A total of 58 patients with PC/PG from TCGA were included in the current study. They included 11 patients with metastasis assigned to the malignant PC/PG group. Among 171 patients with PC/PG derived from COMETE cohort, there were 19 patients with malignant PC/PG. TCGA and COMETE cohort showed no age or gender difference in malignant and benign manifestations (Table 1). The mean follow-up periods were 2460.2 ± 2658.9 days and 1617.6 ± 867.7 days in malignant and benign PC/PG, respectively ($p = 0.320$). The proportion of cases diagnosed with paraganglioma was significantly higher among cases of malignant PC/PG ($p < 0.001$). The size was also significantly greater in malignant PC/PG ($p < 0.001$). The optimal cut-off value was calculated to identify malignancy. According to the ROC curves, the highest accuracy was obtained with a size of 54.5 mm (AUC = 0.778, sensitivity = 66.7%, specificity = 61.6%, and $p < 0.001$) (Figure 3). Dopamine secretion was more frequent in malignant PC/PG, whereas metanephrine secretion was only detected in benign cases of PC/PG (Table 2).

3.2. mRNA Analysis. In TCGA, 6,056 out of 20,531 genes were excluded because at least one sample scored zero value. Based on a comparative analysis of 14,475 genes, 367 upregulated genes were identified while 282 genes were downregulated. A total of 39,534 probes were used to analyze COMETE cohort. Results showed an upregulation of 558 probes and downregulation of 1,132 probes. In both data, the quality control was performed for each gene or probe. The gene expression was analyzed in various ways. Functional annotation analysis was used for gene set enrichment (Figure 4). The top 50 features identified in Gene Set Enrichment Analysis are listed in Supplemental Table 1. Commonly enriched pathways in malignant PC/PG were linked to significant mitosis, metabolic alteration, and cancer signaling (Figure 5). Hierarchical clustering analysis was

Table 1: Clinical demographics of malignant and benign PC/PG cases obtained from the TCGA database and the COMETE cohort.

Characteristic	Malignant (n = 30)	Benign (n = 199)	*p* value
Age (years), mean ± SD	38.9 ± 14.4	43.2 ± 15.7	0.140
Gender, n (%)	30	199	0.432
Male	15 (50.0)	83 (51.1)	
Female	15 (50.0)	116 (48.9)	
Race, n (%)	11	46	0.497
White	10 (90.9)	36 (78.2)	
African-American	1 (9.1)	5 (10.9)	
Asia	0 (0)	5 (10.9)	
Laterality, n (%)	6	41	0.749
Right	2 (33.3)	19 (46.4)	
Left	4 (66.7)	21 (51.2)	
Bilaterality	0 (0)	1 (2.4)	
Diagnosis, n (%)	30	199	<0.001
PC	15 (50.0)	177 (87.2)	
PG	15 (50.0)	22 (12.8)	
Size (mm), mean ± SD	73.4 ± 28.1	46.8 ± 20.2	<0.001
Follow-up (days), mean ± SD	2460.2 ± 2658.9	1617.6 ± 867.7	0.320

PC: pheochromocytoma; PG: paraganglioma.

Table 2: Catecholamine secretion by malignant and benign PC/PG cases derived from TCGA.

Characteristic	Malignant (n = 9)	Benign (n = 40)	*p* value
Biochemical testing			
Normetanephrine	6	34	0.336
Norepinephrine	5	24	1.000
Epinephrine	1	15	0.238
Metanephrine	0	21	0.006
Methoxytyramine	1	0	0.184
Dopamine	4	5	0.046

PC: pheochromocytoma; PG: paraganglioma.

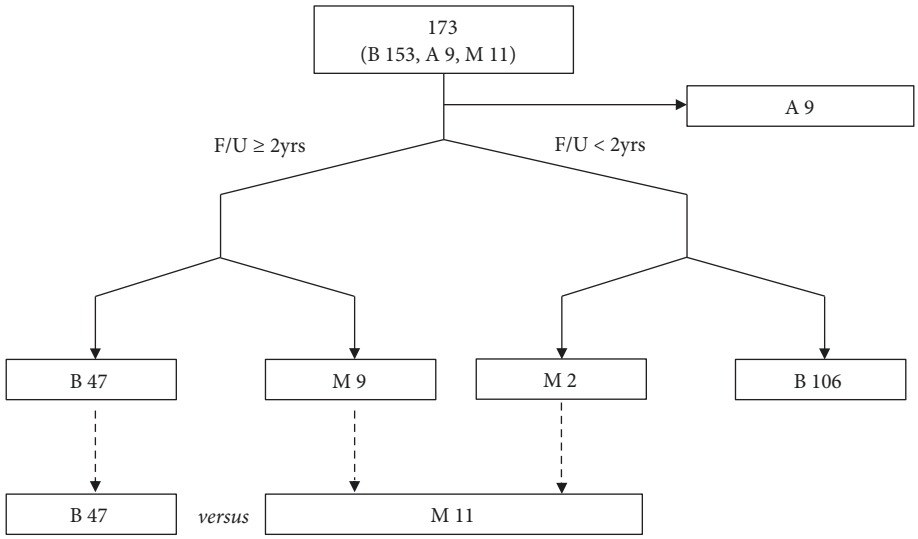

Figure 1: Flow diagram outlining enrollment protocol in TCGA. PC: pheochromocytoma; PG: paraganglioma; M: malignant; A: aggressive; B: benign; F/U: follow-up.

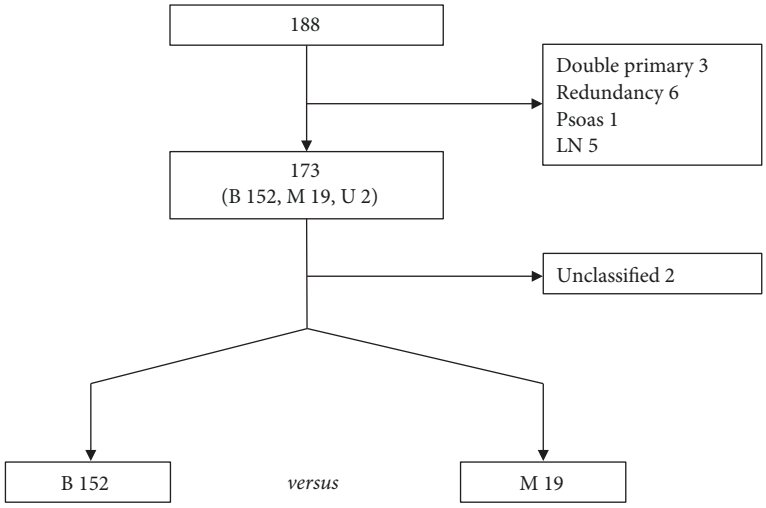

Figure 2: Flow diagram outlining the enrollment protocol in COMETE cohort. PC: pheochromocytoma; PG: paraganglioma; M: malignant; B: benign; U: unclassified; LN: lymph node.

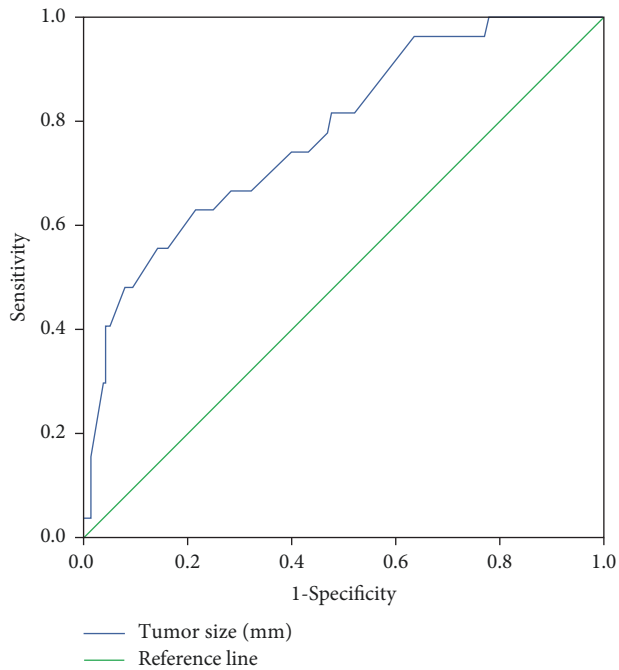

Figure 3: According to the ROC curves, the size of 54.5 mm yielded the highest accuracy in TCGA and COMETE cohort (AUC = 0.778, sensitivity = 66.7%, specificity = 61.6%, and $p < 0.001$). ROC: receiver operating characteristic; AUC: area under the curve.

performed by Euclidean distance and complete linkage. The common up/downregulated differentially expressed genes (DEGs) were extracted from TCGA and COMETE cohort (Supplemental Table 2). The 11 up/downregulated pathways harbored over/underexpressed genes (Table 3). The cyclin and cell cycle regulation as well as the dopamine receptor signaling representing pathways in TCGA and COMETE cohort were displayed in Figure 6. The seven common genes identified were validated in the Dutch cohort (GSE67066). As potential biomarkers, the seven genes in the current study are presented in bold (Supplemental Table 3). Among the seven common genes identified, the overall survival rate in TCGA was significantly correlated with the expression of four genes (*TOP2A*, *ESPL1*, *CDK1*, and *TYMS*) (Figure 7).

4. Discussion

Currently few reliable histopathological criteria predict malignant behavior in PC/PG. Studies to date reported prognostic factors for malignant PC/PG including older age, greater tumor size, extra-adrenal location, elevated dopamine, and synchronous metastasis [13, 14, 19, 25–27]. In the present study, the possible clinical risk factors included dopamine secretion, PG, and greater tumor size. These observations were generally consistent with previous studies. Differences in genomic expression of malignant PC/PG were investigated using data derived from TCGA and COMETE cohort to predict the clinical prognosis. The 11 up/downregulated pathways in malignant PC/PG were significantly associated with the clinical phenotype of increased tumor size and dopamine secretion. Six upregulated and one downregulated genes were significantly enriched in functional annotation pathways. In PC/PG transformed to malignant types, cellular or nuclear proliferation, signaling network, and metabolic changes were essential processes linked to cancer progression. Among the seven common genes, four genes were considerably correlated with overall survival rate.

Grading for adrenal pheochromocytoma and paraganglioma (GAPP) and pheochromocytoma of the adrenal gland scaled score (PASS) have been developed to predict malignancy based on histopathology [28–30]. These two risk stratification systems show several common features, including high cellularity, tumor necrosis, vascular or capsular invasion, and large nest. The recurrent themes carry implied validity. However, these systems are limited intrinsically or due to the absence of consistent validation [28, 30].

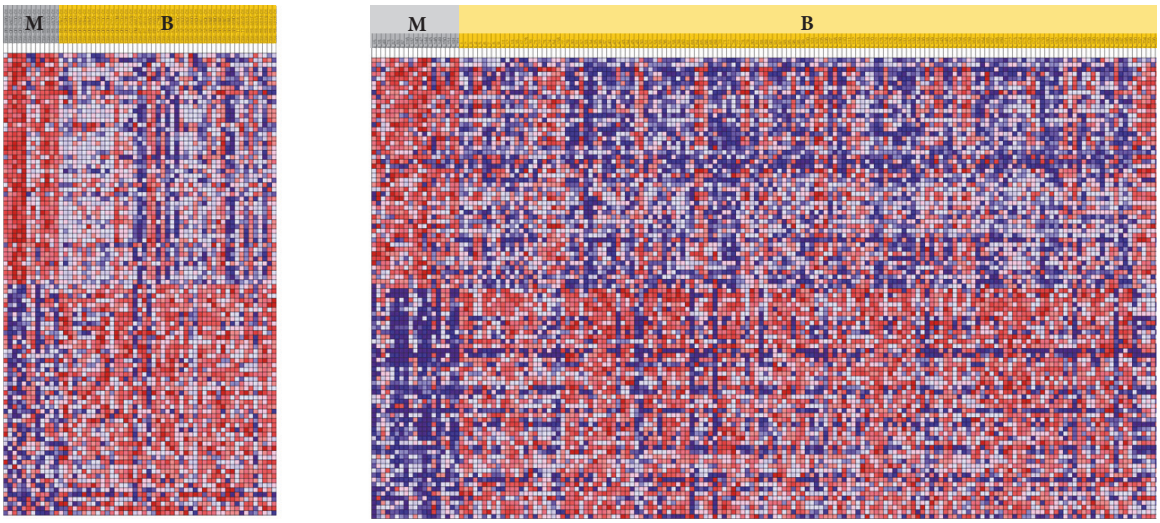

(a) (b)

Figure 4: Gene Set Enrichment Analysis showing the heat map of top 50 features for each phenotype based on metastasis of PC/PG cases in (a) TCGA and (b) COMETE cohort. PC: pheochromocytoma; PG: paraganglioma; M: malignant; B: benign.

Table 3: Ingenuity Canonical Pathways and the corresponding genes in the transcriptome analysis differentiating malignant PC/PG cases in TCGA and COMETE cohort.

Ingenuity Canonical Pathways	Regulation	
	Up	*Down*
Cyclins and Cell Cycle Regulation	*CCNA2, CDK1*	
Dopamine-DARPP32 Feedback in cAMP Signaling		*PRKACB*
Mitotic Roles of Polo-Like Kinase	*CDK1, ESPL1*	
Cell Cycle Control of Chromosomal Replication	*CDK1, CDT1, TOP2A*	
Cardiac β-adrenergic Signaling		*PRKACB*
Dopamine Receptor Signaling		*PRKACB*
Role of CHK Proteins in Cell Cycle Checkpoint Control	*CDK1*	
Pyrimidine Deoxyribonucleotides De Novo Biosynthesis I	*TYMS*	
Salvage Pathways of Pyrimidine Ribonucleotides	*CDK1*	
Protein Kinase A Signaling		*PRKACB*
DNA damage-induced 14-3-3σ Signaling	*CDK1*	

PC: pheochromocytoma; PG: paraganglioma.

In one study, 58 pheochromocytoma samples were analyzed to distinguish malignant samples [31]. Based on lymph node or distant metastasis, 13 samples were classified as malignant. Genome-wide expression profiling was used to select 10 genes among 109 DEGs which were selected. The present study had a similar focus. However, the current study was designed in response to the challenges documented in the 8th edition of the AJCC staging system. Malignant tumors may not be associated with local invasion or locoregional lymph node metastases. Therefore, a stricter definition of malignancy was used to classify patients with PC/PG. Data derived from the two public databases were used for consistency. Even in functionally enriched pathways, each cascade was investigated for common genes. The 11 functional pathways were presumably transformed to malignancy, and included six upregulated and one downregulated genes.

The current results were based on accumulated biological information. These genes were validated in TCGA and COMETE cohort. In other studies, the tumorigenesis of PC/PG was explained via alteration in the three representative molecular signaling pathways including pseudohypoxia signaling, kinase signaling, and *WNT* signaling [18, 20, 21, 32, 33]. Activation of effector molecules in pseudohypoxia signaling is triggered by genetic mutations involving the degradation of hypoxia-inducible factor 1/2α or Krebs cycle function, such as succinate dehydrogenase genes (*SDHx*), *VHL*, or *EPAS1* [34]. These changes suggest increased levels of angiogenesis and enable hematogenous dissemination [35, 36]. Hyperactive kinase signaling is induced by mutations involving genes associated with mitogen-activated protein kinase, such as tumor suppressor genes (*NF1, TMEM127, MAX,* and *KIF1Bβ*), *RET,* or *HRAS*, which promoted growth

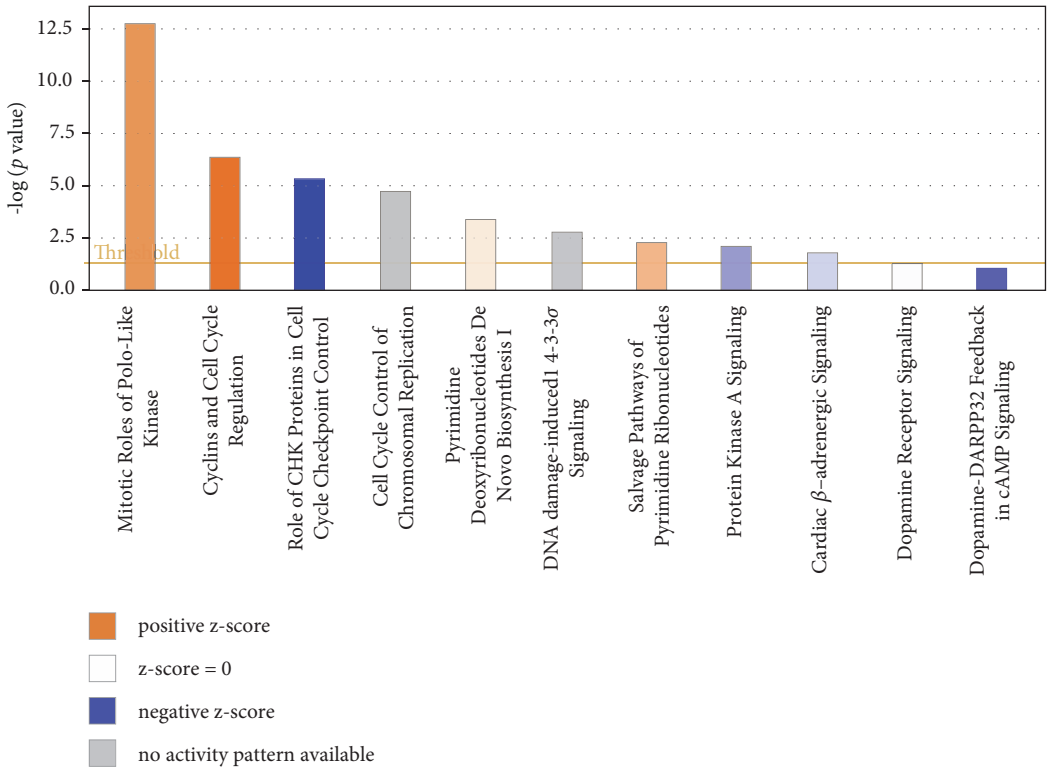

(a)

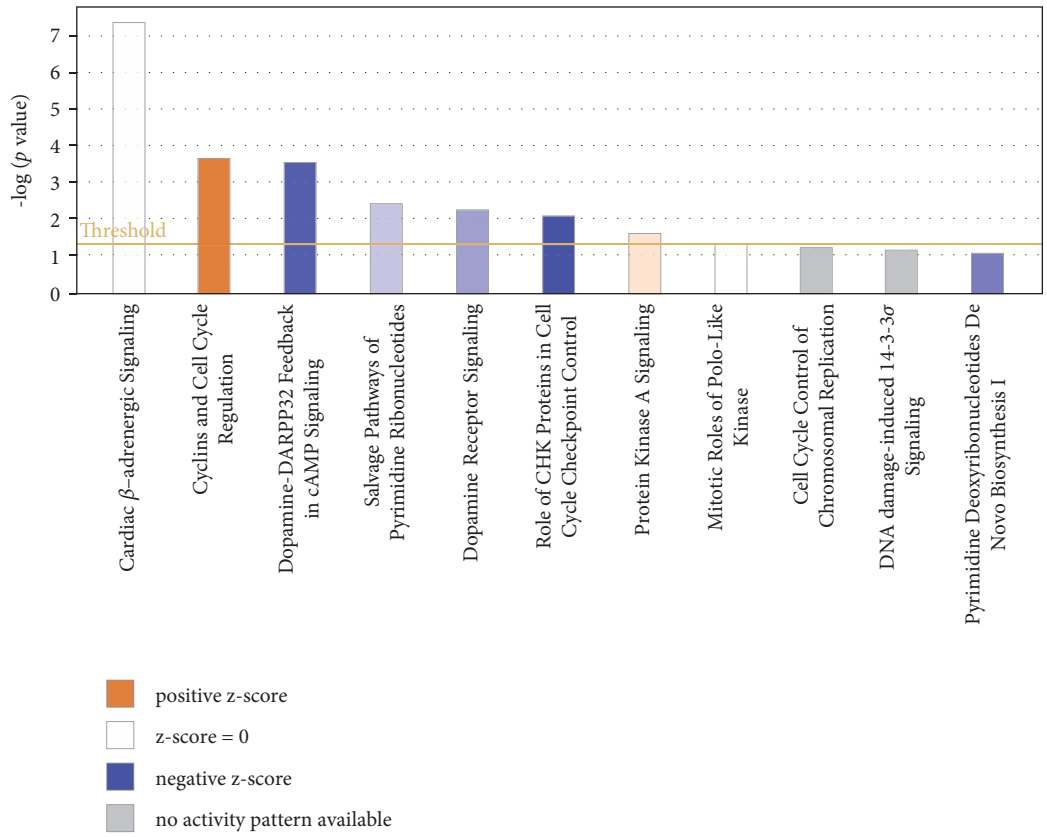

(b)

Figure 5: Ingenuity Canonical Analysis showing 11 pathways harboring the corresponding genes in the transcriptome analysis to differentiate malignant PC/PG in (a) TCGA and (b) COMETE cohort. PC: pheochromocytoma; PG: paraganglioma.

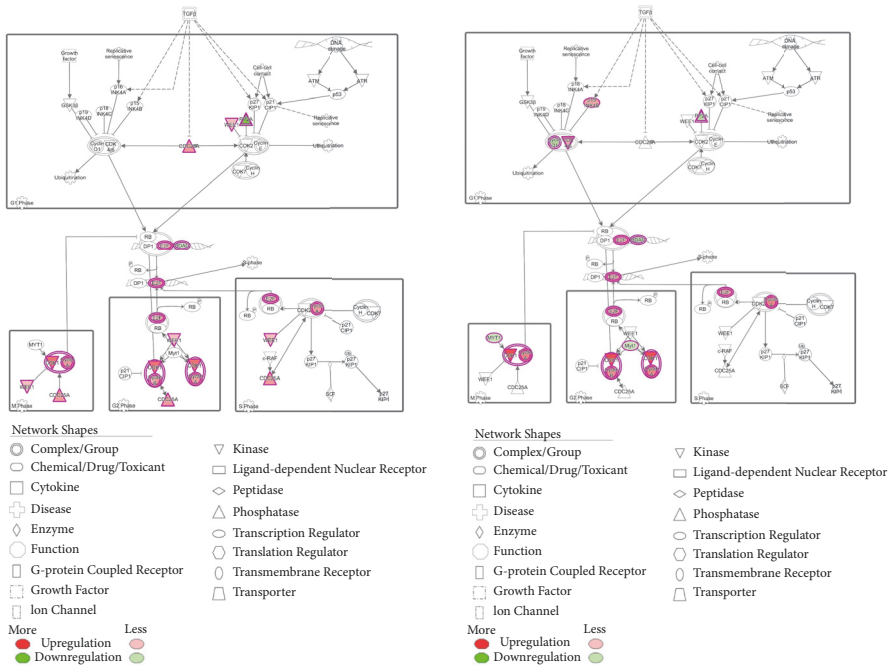

Figure 6: Continued.

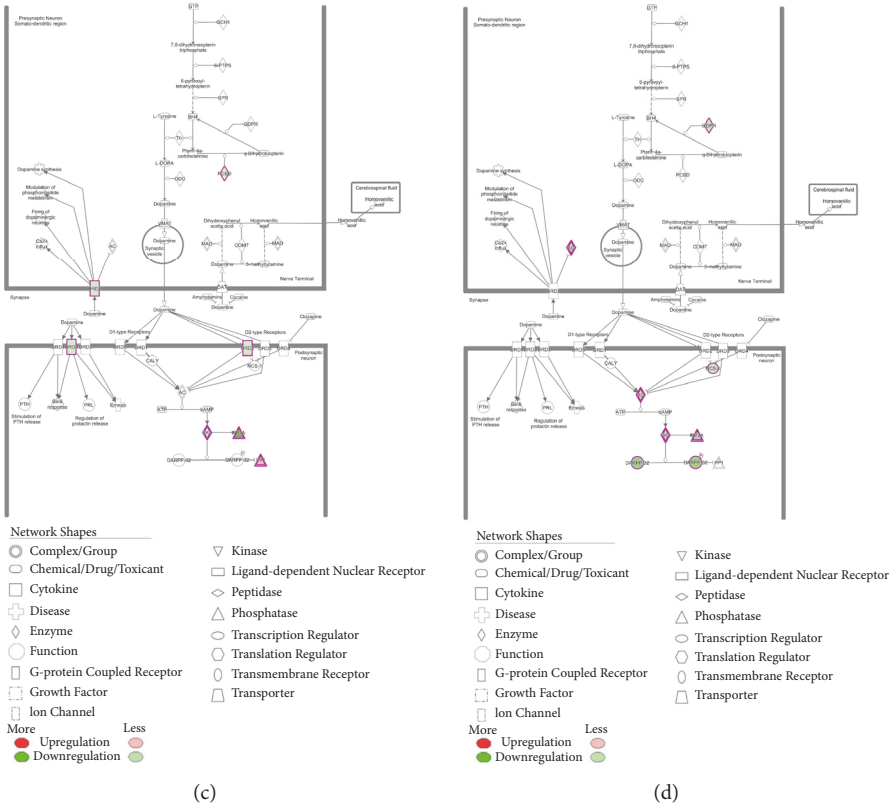

Figure 6: Up/downregulated genes in enriched pathways: cyclins and cell cycle of (a) TCGA and (b) COMETE cohort and dopaminergic synapse of (c) TCGA and (d) COMETE cohort.

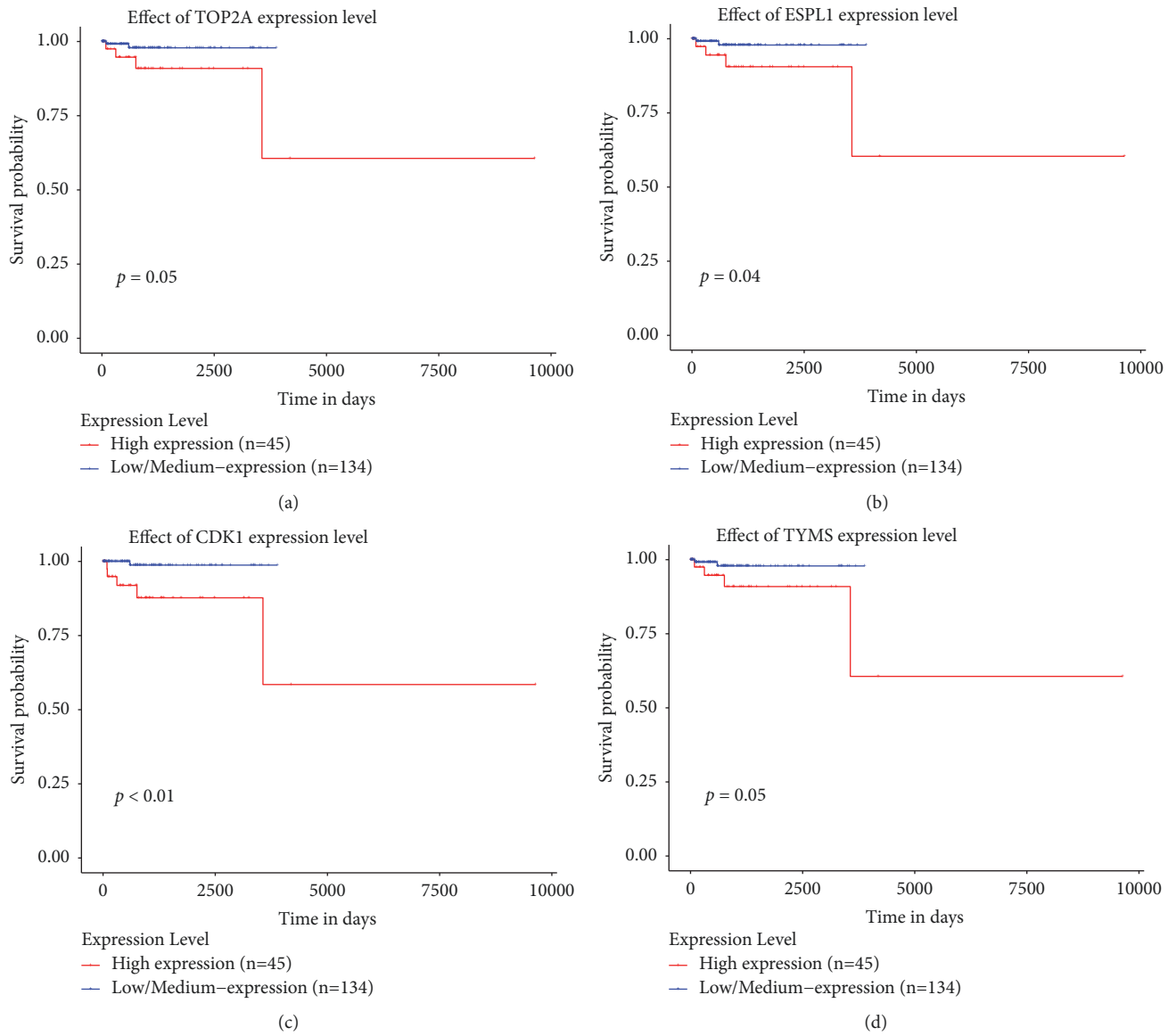

Figure 7: When the identified genes were analyzed in UALCAN, overall survival rate in TCGA was considerably significantly with four genes: (a) *TOP2A*, (b) *ESPL1*, (c) *CDK1*, and (d) *TYMS*.

independence of extracellular signals [35, 37, 38]. Additionally, upregulated *WNT* signaling has been recently reported in genetic alterations of *MAML3* and *CSDE1* [20].

In the present study, DEGs were enriched in 11 presumptive pathways that interacted closely with the three known molecular pathways mentioned above. Further, the 11 presumptive pathways mediated malignant transformation, including cellular or nuclear proliferation, signaling, and metabolic changes predicting cancer progression. However, whether these pathways directly mediated metastasis or the by-product circuits remains to be investigated.

Among the 11 pathways, six common genes (*TOP2A, ESPL1, CDK1, TYMS, CDT1,* and *CCNA2*) were differentially overexpressed, and one common gene (*PRKACB*) was underexpressed in malignant PC/PG. These genes play a role in cell cycle, cell signaling, and tumor metabolism of malignant PC/PG as well as in other cancers. These six overexpressed genes play a critical role in signaling pathways or cell proliferation, which can increase the tumor size in malignant PC/PG as shown in Table 1. The underexpressed gene was correlated with signaling pathways or metabolic changes, which may lead to differential catecholamine secretion as shown in Table 2. Abnormal *TOP2A* overexpression leads to chromosomal instability. *ESPL1* plays a pivotal role in chromatid separation. The overexpression of *CDK1, TYMS, CDT1,* and *CCNA2* and the underexpression of *PRKACB* were associated with tumorigenesis, defective cell signaling, or aberrant metabolism in other cancers [39]. These genes served as prognostic genes for malignant PC/PG in this study.

Germline mutations have been reported in 20-41% cases of PC/PG [3]. Comprehensive analyses have implicated germline mutations involving *SDHB*, *FH*, *MAX*, and

SLC25A11 in the origin and development of malignant PC/PG [40–43]. It is generally recognized that PC/PG carrying germline mutations of *SDHB* show a higher rate of metastasis [44]. The *SDHB* mutation in Krebs cycle impairs glucose metabolism, leading to inhibition of 2-oxoglutarate-dependent histone and DNA demethylase enzymes. The mutation rate and the spectrum of malignant PC/PG were not comparable in these different cohorts. The germline mutation of *SDHB* was significantly susceptible to malignancy in TCGA and COMETE cohort ($p = 0.0049$ and $p < 0.001$, respectively). Mutations involving *SDHx* or *FH* lead to DNA hypermethylation, explaining both the tumor-suppressive role of these genes and the phenotypic characteristics [45]. In particular, the malignancy of *SDHB* mutation is attributed to severe epigenetic silencing of genes involved in cell differentiation and epithelial-to-mesenchymal transition. *RDBP* hypermethylation may alter transcriptional networks involving apoptosis, invasion, and maintenance of DNA integrity [46].

To the best of our knowledge, this study is the first transcriptome analysis identifying prognostic genes for malignant PC/PG defined in the 8th edition of the AJCC staging system. We identified potential pathways leading to malignant transformation of PC/PG and subsequently up/downregulated genes in malignant PC/PG. Specific genes in the current study may be used for the development of gene expression classifier [47]. The development of gene expression classifier is expected to improve the diagnostic accuracy and treatment decision. Novel molecular therapeutics can be developed based on the results of the current study.

The current study has a few limitations. First, no comprehensive analysis of microRNA, DNA methylation, copy-number variation, mutation, or protein expression was carried out to establish the complete signature of malignant PC/PG. Second, only two proven databases were used in the present study. Identification of databases for genomic analysis is difficult because PC/PG is a rare disease. Third, as a general limitation of public data analysis, the present study was based on limited data provided.

In conclusion, data from the TCGA database and the COMETE cohort showed differences in mRNA expression between malignant and benign PC/PG. Improved recognition of prognostic genes based on our analyses will facilitate appropriate diagnosis and treatment of malignant PC/PG.

Data Availability

The data used to support the findings of this study are available from the corresponding author upon request.

Conflicts of Interest

No potential conflicts of interest relevant to this article were reported.

Acknowledgments

Macrogen Inc. (Seoul, Korea) provided technical services for genetic analysis. The results reported here were based partly upon data generated by TCGA and European Bioinformatics Institute. This study was funded by Hallym University Research (HURF-2017-41).

Supplementary Materials

Supplemental Table 1: the top 50 features of Gene Set Enrichment Analysis based on metastasis in pheochromocytoma/paraganglioma from TCGA and COMETE cohort. *Supplemental Table 2:* the common differentially expressed (up/downregulated) genes (DEGs) extracted from TCGA and COMETE cohort. *Supplemental Table 3:* the 34 common differentially expressed (up/downregulated) genes (DEGs) validated in GSE67066 cohort. *(Supplementary Materials)*

References

[1] J. W. M. Lenders, G. Eisenhofer, M. Mannelli, and K. Pacak, "Phaeochromocytoma," *The Lancet*, vol. 366, no. 9486, pp. 665–675, 2005.

[2] E. P. Corssmit and J. A. Romijn, "Clinical management of paragangliomas," *European Journal of Endocrinology*, vol. 171, no. 6, pp. R231–R243, 2014.

[3] C. M. Kiernan and C. C. Solórzano, "Pheochromocytoma and paraganglioma: diagnosis, genetics, and treatment," *Surgical Oncology Clinics of North America*, vol. 25, no. 1, pp. 119–138, 2016.

[4] K. E. Joynt, J. J. Moslehi, and K. L. Baughman, "Paragangliomas: etiology, presentation, and management," *Cardiology in Review*, vol. 17, no. 4, pp. 159–164, 2009.

[5] E. L. Bravo and R. Tagle, "Pheochromocytoma: State-of-the-art and future prospects," *Endocrine Reviews*, vol. 24, no. 4, pp. 539–553, 2003.

[6] J. W. M. Lenders, Q.-Y. Duh, and G. Eisenhofer, "Pheochromocytoma and paraganglioma : an endocrine society clinical practice guideline," *The Journal of Clinical Endocrinology & Metabolism*, vol. 99, no. 6, pp. 1915–1942, 2014.

[7] A. Chrisoulidou, G. Kaltsas, I. Ilias, and A. B. Grossman, "The diagnosis and management of malignant phaeochromocytoma and paraganglioma," *Endocrine-Related Cancer*, vol. 14, no. 3, pp. 569–585, 2007.

[8] E. Baudin, M. A. Habra, F. Deschamps et al., "Therapy of endocrine disease: treatment of malignant pheochromocytoma and paraganglioma," *European Journal of Endocrinology*, vol. 171, no. 3, pp. R111–R122, 2014.

[9] R. Adjallé, P. F. Plouin, K. Pacak, and H. Lehnert, "Treatment of malignant pheochromocytoma," *Hormone and Metabolic Research*, vol. 41, no. 9, pp. 687–696, 2009.

[10] A. S. Tischler, K. Pacak, and G. Eisenhofer, "The adrenal medulla and extra-adrenal paraganglia: Then and now," *Endocrine Pathology*, vol. 25, no. 1, pp. 49–58, 2014.

[11] E. E. Elder, G. Elder, and C. Larsson, "Pheochromocytoma and functional paraganglioma syndrome: No longer the 10% tumor," *Journal of Surgical Oncology*, vol. 89, no. 3, pp. 193–201, 2005.

[12] K. F. Andersen, R. Altaf, A. Krarup-Hansen et al., "Malignant pheochromocytomas and paragangliomas - The importance of

a multidisciplinary approach," *Cancer Treatment Reviews*, vol. 37, no. 2, pp. 111–119, 2011.

[13] L. D. R. Thompson, "Pheochromocytoma of the adrenal gland scaled score (PASS) to separate benign from malignant neoplasms: a clinicopathologic and immunophenotypic study of 100 cases," *The American Journal of Surgical Pathology*, vol. 26, no. 5, pp. 551–566, 2002.

[14] P. Goffredo, J. A. Sosa, and S. A. Roman, "Malignant pheochromocytoma and paraganglioma: A population level analysis of long-term survival over two decades," *Journal of Surgical Oncology*, vol. 107, no. 6, pp. 659–664, 2013.

[15] O. Gimm, C. DeMicco, A. Perren, F. Giammarile, M. K. Walz, and L. Brunaud, "Malignant pheochromocytomas and paragangliomas: A diagnostic challenge," *Langenbeck's Archives of Surgery*, vol. 397, no. 2, pp. 155–177, 2012.

[16] R. R. De Krijger, F. H. Van Nederveen, E. Korpershoek, and W. N. M. Dinjens, "New developments in the detection of the clinical behavior of pheochromocytomas and paragangliomas," *Endocrine Pathology*, vol. 17, no. 2, pp. 137–141, 2006.

[17] T. Scholz, C. Schulz, S. Klose, and H. Lehnert, "Diagnostic management of benign and malignant pheochromocytoma," *Experimental and Clinical Endocrinology & Diabetes*, vol. 115, no. 03, pp. 155–159, 2007.

[18] P. Björklund, K. Pacak, and J. Crona, "Precision medicine in pheochromocytoma and paraganglioma: current and future concepts," *Journal of Internal Medicine*, vol. 280, no. 6, pp. 559–573, 2016.

[19] F. Feng, Y. Zhu, X. Wang et al., "Predictive factors for malignant pheochromocytoma: analysis of 136 patients," *The Journal of Urology*, vol. 185, no. 5, pp. 1583–1589, 2011.

[20] L. Fishbein, I. Leshchiner, and V. Walter, "Comprehensive molecular characterization of pheochromocytoma and paraganglioma," *Cancer Cell*, vol. 31, no. 2, pp. 181–193, 2017.

[21] L. J. Castro-Vega, E. Letouzé, N. Burnichon et al., "Multi-omics analysis defines core genomic alterations in pheochromocytomas and paragangliomas," *Nature Communications*, vol. 6, no. 1, 2015.

[22] N. Burnichon, L. Vescovo, L. Amar et al., "Integrative genomic analysis reveals somatic mutations in pheochromocytoma and paraganglioma," *Human Molecular Genetics*, vol. 20, no. 20, Article ID ddr324, pp. 3974–3985, 2011.

[23] L. Evenepoel, F. H. Van Nederveen, L. Oudijk et al., "Expression of contactin 4 is associated with malignant behavior in pheochromocytomas and paragangliomas," *The Journal of Clinical Endocrinology & Metabolism*, vol. 103, no. 1, pp. 46–55, 2018.

[24] D. S. Chandrashekar, B. Bashel, S. A. H. Balasubramanya et al., "UALCAN: a portal for facilitating tumor subgroup gene expression and survival analyses," *Neoplasia (United States)*, vol. 19, no. 8, pp. 649–658, 2017.

[25] O. Hamidi, W. F. Young, N. M. Iñiguez-Ariza et al., "Malignant pheochromocytoma and paraganglioma: 272 patients over 55 years," *The Journal of Clinical Endocrinology & Metabolism*, vol. 102, no. 9, pp. 3296–3305, 2017.

[26] Y. M. Choi, T.-Y. Sung, W. G. Kim et al., "Clinical course and prognostic factors in patients with malignant pheochromocytoma and paraganglioma: A single institution experience," *Journal of Surgical Oncology*, vol. 112, no. 8, pp. 815–821, 2015.

[27] M. Ayala-Ramirez, L. Feng, M. M. Johnson et al., "Clinical risk factors for malignancy and overall survival in patients with pheochromocytomas and sympathetic paragangliomas: primary tumor size and primary tumor location as prognostic indicators," *The Journal of Clinical Endocrinology & Metabolism*, vol. 96, no. 3, pp. 717–725, 2011.

[28] A. S. Tischler and R. R. De Krijger, "Pathology of pheochromocytoma and paraganglioma," *Endocrine-Related Cancer*, vol. 22, no. 4, pp. T123–T133, 2015.

[29] N. Kimura, T. Watanabe, T. Noshiro, S. Shizawa, and Y. Miura, "Histological grading of adrenal and extra-adrenal pheochromocytomas and relationship to prognosis: A clinicopathological analysis of 116 adrenal pheochromocytomas and 30 extra-adrenal sympathetic paragangliomas including 38 malignant tumors," *Endocrine Pathology*, vol. 16, no. 1, pp. 23–32, 2005.

[30] G. Eisenhofer and A. S. Tischler, "Neuroendocrine cancer: Closing the GAPP on predicting metastases," *Nature Reviews Endocrinology*, vol. 10, no. 6, pp. 315-316, 2014.

[31] I. Suh, D. Shibru, G. Eisenhofer et al., "Candidate genes associated with malignant pheochromocytomas by genome-wide expression profiling," *Annals of Surgery*, vol. 250, no. 6, pp. 983–990, 2009.

[32] J. Favier, L. Amar, and A.-P. Gimenez-Roqueplo, "Paraganglioma and phaeochromocytoma: from genetics to personalized medicine," *Nature Reviews Endocrinology*, vol. 11, no. 2, pp. 101–111, 2015.

[33] L. Santarpia, M. A. Habra, and C. Jiménez, "Malignant pheochromocytomas and paragangliomas: Molecular signaling pathways and emerging therapies," *Hormone and Metabolic Research*, vol. 41, no. 9, pp. 680–686, 2009.

[34] F. Khatami, M. Mohammadamoli, and S. M. Tavangar, "Genetic and epigenetic differences of benign and malignant pheochromocytomas and paragangliomas (PPGLs)," *Endocrine Regulations*, vol. 52, no. 1, pp. 41–54, 2018.

[35] J. Favier and A.-P. Gimenez-Roqueplo, "Pheochromocytomas: the (pseudo)-hypoxia hypothesis," *Best Practice & Research Clinical Endocrinology & Metabolism*, vol. 24, no. 6, pp. 957–968, 2010.

[36] H. M. Rossitti, P. Söderkvist, and O. Gimm, "Extent of surgery for phaeochromocytomas in the genomic era," *British Journal of Surgery*, vol. 105, no. 2, pp. e84–e98, 2018.

[37] A.-P. Gimenez-Roqueplo, P. L. Dahia, and M. Robledo, "An update on the genetics of paraganglioma, pheochromocytoma, and associated hereditary syndromes," *Hormone and Metabolic Research*, vol. 44, no. 5, pp. 328–333, 2012.

[38] S. O. Zhikrivetskaya, A. V. Snezhkina, A. R. Zaretsky et al., "Molecular markers of paragangliomas/pheochromocytomas," *Oncotarget* , vol. 8, no. 15, pp. 25756–25782, 2017.

[39] S. Fan, Y. Wang, Z. Zhang et al., "High expression of glutamate-ammonia ligase is associated with unfavorable prognosis in patients with ovarian cancer," *Journal of Cellular Biochemistry*, vol. 119, no. 7, pp. 6008–6015, 2018.

[40] L. Amar, E. Baudin, N. Burnichon et al., "Succinate dehydrogenase B gene mutations predict survival in patients with malignant pheochromocytomas or paragangliomas," *The Journal of Clinical Endocrinology & Metabolism*, vol. 92, no. 10, pp. 3822–3828, 2007.

[41] L. J. Castro-Vega, A. Buffet, A. A. De Cubas et al., "Germline mutations in FH confer predisposition to malignant pheochromocytomas and paragangliomas," *Human Molecular Genetics*, vol. 23, no. 9, Article ID ddt639, pp. 2440–2446, 2014.

[42] B. Bausch, F. Schiavi, Y. Ni et al., "Clinical characterization of the pheochromocytoma and paraganglioma susceptibility genes SDHA, TMEM127, MAX, and SDHAF2 for gene-informed prevention," *JAMA Oncology*, vol. 3, no. 9, pp. 1204–1212, 2017.

[43] A. Buffet, A. Morin, L.-J. Castro-Vega et al., "Germline mutations in the mitochondrial 2-oxoglutarate/malate carrier SLC25A11 gene confer a predisposition to metastatic paragangliomas," *Cancer Research*, vol. 78, no. 8, pp. 1914–1922, 2018.

[44] J. Turchini, V. K. Y. Cheung, A. S. Tischler, R. R. De Krijger, and A. J. Gill, "Pathology and genetics of phaeochromocytoma and paraganglioma," *Histopathology*, vol. 72, no. 1, pp. 97–105, 2018.

[45] E. Letouzé, C. Martinelli, C. Loriot et al., "SDH mutations establish a hypermethylator phenotype in paraganglioma," *Cancer Cell*, vol. 23, no. 6, pp. 739–752, 2013.

[46] A. A. De Cubas, E. Korpershoek, L. Inglada-Pérez et al., "DNA methylation profiling in pheochromocytoma and paraganglioma reveals diagnostic and prognostic markers," *Clinical Cancer Research*, vol. 21, no. 13, pp. 3020–3030, 2015.

[47] R. Simon, "Roadmap for developing and validating therapeutically relevant genomic classifiers," *Journal of Clinical Oncology*, vol. 23, no. 29, pp. 7332–7341, 2005.

Hindawi
International Journal of Endocrinology
Volume 2019, Article ID 5303765, 9 pages
https://doi.org/10.1155/2019/5303765

Research Article

Causes and Follow-Up of Central Diabetes Insipidus in Children

Wendong Liu,[1] Jing Hou,[1] Xiuqin Liu,[1] Limin Wang,[1] and Guimei Li[2]

[1]*Department of Pediatrics, Qingdao Municipal Hospital Affiliated to Qingdao University, Qingdao, China*
[2]*Department of Pediatrics, Shandong Provincial Hospital Affiliated to Shandong University, Jinan, China*

Correspondence should be addressed to Guimei Li; lgmusa2015@163.com

Received 7 November 2018; Revised 19 February 2019; Accepted 24 February 2019; Published 27 March 2019

Guest Editor: Giampaolo Papi

Objective. To identify the causes of central diabetes insipidus (CDI) by evaluating the values of magnetic resonance imaging (MRI) in the diagnosis of pediatric CDI, providing evidence for the clinical diagnosis and treatment of CDI. *Methods*. Seventy-nine patients with CDI (CDI group) hospitalized from July 2012 to March 2017 and 43 healthy children (control group) were enrolled in this study. All cases underwent MRI examination including T1-weighted three-dimensional magnetization-prepared rapid gradient-echo (T1WI-3D-MP RAGE) imaging sequences. The pituitary volume, the signal intensity of posterior pituitary, and the morphology of pituitary stalk were measured between two groups. The medical history, urine testing, imaging of hypothalamic-pituitary region, and hormone levels were also recorded. *Results*. Age and gender were matched between the CDI and control groups. The height and BMI in the CDI group were less and the urine volume in 24 h was higher than those in the control group. The signal intensity of the posterior pituitary was higher in the control group, whereas the pituitary volume was smaller in the CDI group. In the CDI group, 44 cases presented with morphological changes of the pituitary stalk. Clinical symptoms mainly included polydipsia, polyuria, short stature, and vomiting. All patients were confirmed by water deprivation vasopressin test. Forty-four CDI children were associated with hypopituitarism, including 33 cases of PSIS with multiple pituitary hormone deficiencies (MPHD) and 11 cases of growth hormone deficiency (IGHD). The pituitary volume in the cases of pituitary stalk interruption syndrome (PSIS) with MPHD was smaller than that in the IGHD patients. *Conclusions*. The signal intensity ratio of the posterior lobe, pituitary volume, and the morphology of pituitary stalk on T1WI-3D-MP RAGE image contribute to the diagnosis of CDI.

1. Introduction

Central diabetes insipidus (CDI) is characterized by polyuria and polydipsia and caused by deficiency of arginine vasopressin (AVP), an antidiuretic hormone which acts on V2 receptors in the kidney to promote reabsorption of free water [1, 2]. Patients with CDI may have anterior pituitary hypofunction, complicated with growth hormone deficiency alone or multiple pituitary hormone deficiencies, leading to abnormalities in the anterior pituitary hormone axis and affecting the pediatric growth and development. Therefore, unravelling the etiology and comprehensive assessment of the condition should be performed for early intervention treatment.

With the development of laboratory examinations and imaging technologies, the diagnosis and etiological identification of CDI have become mature. Magnetic resonance imaging (MRI) of the hypothalamic-pituitary region can visually show the lesions, adjacent structures, and the abnormality of hypothalamic-neuronal system, which plays an irreplaceable role in the diagnosis of CDI [3, 4]. However, due to the small structures of the hypothalamus and pituitary gland, the abnormalities of idiopathic CDI patients cannot be identified with conventional MRI due to low resolution [5]. Nevertheless, T1-weighted three-dimensional magnetization-prepared rapid acquisition gradient-echo (T1WI-3D-MP RAGE) sequence can contribute to the etiological diagnosis of CDI. The T1WI-3D-MP RAGE scan is a newly developed rapid T1-weighted imaging sequence which can be used for continuous thin-slice scanning, reducing partial volume effects and particularly reducing postcranial concave artifact interference [6, 7]. It is helpful to show small lesions in details [8], especially the pituitary stalk and the posterior pituitary. It is simple, feasible, and practical to utilize this sequence to display the hypothalamic-

Table 1: Scan parameters of each sequence for MRI examination.

	TR (ms)	TE (ms)	FA	Thickness/layer spacing (mm)	Matrix	FOV	Scanning time (min)
T1WI-3D-MP RAGE	10.5	4.0	12°	1/0	256 × 256	256 × 256	10.0
T2WI sweep	4000.0	100.0	—	3/0	256 × 256	256 × 256	2.6
T1 enhanced inspection	200.0	9.1	—	3/0	256 × 256	256 × 256	1.2

Abbreviation: TR: time repetition; TE: time echo; FOV: field of view.

pituitary region. T1WI-3D-MP RAGE sequence is a new sequence, and its clinical application value remains to be confirmed by more studies. The application of this sequence in the hypothalamic-pituitary zone will allow its advantages to be exploited and may provide the basis for the optimization of CDI imaging protocols.

In this study, the saddle area of 79 CDI patients (CDI group) and 43 normal children was collected (control group). The posterior pituitary signal intensity and pituitary stalk diameter were measured and compared between the two groups. The high-resolution T1WI-3D-MP RAGE imaging combined with MRI, analysis of hormonal changes, and long-term follow-up were conducted in children with different causes of CDI, providing an objective basis for timely diagnosis of CDI, assessment of disease condition, and assessment of clinical prognosis.

2. Materials and Methods

2.1. Subjects. Seventy-nine patients eligible for the criteria of CDI admitted to the Department of Pediatrics and Pediatric Endocrinology, Shandong Provincial Hospital, from July 2012 to March 2017 were selected for the CDI group. Forty-three gender- and age-matched normal children were assigned into the control group.

Inclusion criteria are as follows: (1) polydipsia and polyuria, urine output > 3000 ml/m^2 within 24 h, or >200 ml/h or >6 ml/kg/h lasting for >24 h; urine specific gravity ≤ 1.005, urine osmotic pressure ≤ 200 mOsm/kg·H_2O; plasma osmolality ≥ 300 mOsm/kg·H_2O; urine osmolality/-blood osmotic pressure < 1; (2) water deprivation test: dehydration symptoms after 4-6 h of water deprivation, constant urine volume, urine specific gravity ≤ 1.015, urine osmotic pressure ≤ plasma osmotic pressure; (3) pituitary vasopressin test: rapid increase in urine specific gravity ≥ 1.018, urinary osmotic pressure rise > 9%, urine osmotic pressure/plasma osmotic pressure > 1; and (4) plasma vasopressin determination: AVP value less than normal (normal 1-1.5 ng/l).

Exclusion criteria are as follows: (1) trauma- or surgery-induced transient diabetes insipidus; (2) water pressure test prompted for mental polydipsia, NDI; (3) abnormal heart and kidney function; and (4) MRI images that did not meet diagnostic requirements.

2.2. MRI Examination. A Siemens 3.0 T superconducting MRI scanner was used. All patients underwent pituitary T1WI-3D-MP RAGE scans with sagittal and coronal T2WI plain scans, and gadolinium diethylenetriamine-pentaacetic acid (Gd-DTPA) as contrast agent was used at a dose of 0.1 mmol/kg. The enhanced scan was performed immediately after pushing the contrast agent. Scan parameters in each sequence for the enhanced MRI examination of the hypothalamic-pituitary region are shown in Table 1.

2.3. Data Acquisition and Analysis. The family history, chief complaints, gender, age and duration of onset, water deprivation vasopressin test results, and laboratory test results were recorded for all patients with CDI. The obtained data were analyzed and compared between two groups.

2.4. Urine and Blood Tests. 24-hour urine volume was monitored, and urine specific gravity, urine osmolality, blood Na^+, and blood osmotic pressure were measured.

2.5. Water Deprivation Test. The water deprivation test can roughly distinguish between CDI and mental polydipsia. Active water restriction was performed for a period of time before the experiment. Complete water deprivation was performed in the evening of the day after the start of the trial, and some subjects could not tolerate water withdrawal from 4 am. The clinical observation of the water deprivation test was performed at 8 o'clock in the morning. The measurement indicators included body weight, heart rate, blood pressure, urine volume, urine specific gravity, urine osmotic pressure, blood Na^+, and blood osmotic pressure. After water deprivation, the urine output was not significantly reduced, with clear urine, mental irritability, elevated body temperature, weight loss, urine osmotic pressure < osmotic pressure, and elevated blood osmolality (>305 mOsm/kg·H_2O could terminate the test), who were DI, and urine osmotic pressure of complete diabetes insipidus was less than blood osmotic pressure, and urine osmotic pressure of partial diabetes insipidus was less than blood osmotic pressure. Some children had obvious polyuria and polydipsia during the day, but enuresis nocturna was normal, there were no signs of water shortage, the basic blood sodium was reduced or the normal lower limit, the urine output was reduced after the water deprivation test, the urine became yellow, the urine osmotic pressure and the urine specific gravity were elevated, SG was above 1.018, weight loss was slight, serum sodium and osmotic pressure remained normal, and preliminary consideration was given to psychogenic polydipsia (PP).

2.6. Vasopressin Test. Water deprivation vasopressin test combined with MRI was used to identify CDI and NDI. After the water deprivation test, when patient's urine volume, urine specific gravity, and urine osmotic pressure were stable, the patient was injected with 5 units of pituitary vasopressin (children 6 units/m^2); and the urine volume, urine specific gravity, and urine osmotic pressure were observed. After the injection of vasopressin, urine output in CDI was

decreased, urine specific gravity and osmotic pressure were increased, and the response in NDI was not obvious.

2.7. Anterior Pituitary Functional Examination and Other Examinations. Anterior pituitary function: (1) two growth hormone (GH) stimulation experiments were done: insulin hypoglycemic GH stimulation test and levodopa (L-DOPA) or arginine (ARG) GH stimulation test. The arginine test (0.5 g/kg, maximum 30 g) could be combined with levodopa (10 mg/kg, maximum 0.5 g), and insulin-induced hypoglycemia (0.075-0.1 u/kg) stimulation test was required for the cortisol challenge test. Blood was drawn at 0, 30, 60, 90, and 120 min, and GH was measured. At 0 min, insulin-like growth factor 1 (IGF-1) was added. After stimulation, GH secretion > 10 μg/l (10 ng/ml) was a normal response, <5 μg/l (5 ng/ml) was complete GH deficiency, and 5-10 ng/ml was partial GH deficiency. (2) Pituitary-thyroid axis function: determination of thyroid-stimulating hormone (TSH), T3, and T4. Patients with free T4 < 12.0 pmol/l and no increase of TSH (TSH < 5 uIU/ml) could be diagnosed as secondary hypothyroidism (TSHD). (3) Pituitary-adrenal axis function: the diagnostic criteria for secondary adrenocortical insufficiency (ACTHD) were that cortisol was less than 138 nmol/l at 8 o'clock in the morning or cortisol was lower than 550 nmol/l in insulin-induced hypoglycemia but adrenocorticotropic hormone (ACTH) was not significantly increased. (4) Pituitary-gonadal axis function: determination of follicle-stimulating hormone (FSH), luteinizing hormone (LH), estradiol (E2), testosterone (TO), and prolactin (PRL). The diagnostic criteria for hypogonadism were that the basal level of gonadotropin (FSH, LH) was lower than the normal detection limit (0.1 mIU/ml) or that the LH peak in the GnRH stimulation test was less than 2.8 mIU/ml, with or without FSH peak < 3.7 mIU/ml; LH peaks in peak adolescents undergoing GnRH stimulation were less than 5 mIU/ml; peak of LH/FSH was less than 0.6. (5) Serum prolactin (PRL) levels: diagnostic criterion for hyperprolactinemia was that PRL was higher than 25 ng/ml; the diagnostic criterion for hypoprolactinemia was that PRL was less than 5 ng/ml.

Patients with space-occupying lesions in the sellar area or thickening of the pituitary stalk should also undergo a systemic radionuclide bone scan to assist in the diagnosis of Langerhans cell histiocytosis (LCH) and be diagnosed with Langerhans cell tissue cells detected by a puncture smear from the skin with a hemorrhagic papule or skeletal lesion. Routine determination of alpha-fetoprotein (AFP), human chorionic gonadotropin (β-HCG), and carcinoembryonic antigen (CEA) was used to assist in the diagnosis of germ cell tumors.

2.8. Pituitary-Related Index Measurements and Diagnostic Standards on MRI Images. The T1WI-3D-MP RAGE was measured and averaged by three observers, and the image was magnified several times. The measured data were statistically compared between the CDI and control groups.

(1) Measurement of Pituitary Volume. The pituitary morphology was observed. In the median sagittal position, the height of the central pituitary and the longest diameter before and after the pituitary were measured. The width of the pituitary was measured at the central coronal position. The volume of the pituitary was calculated based on the volume of the pituitary = 1/2 (long diameter × high diameter × wide diameter).

(2) Measurement of Posterior Pituitary Signal. The position and size of the posterior pituitary were carefully observed, and the posterior pituitary signal intensity and the pons signal were measured in the median sagittal position. The region of interest was located posterior to the pituitary or the inner side of the pons. The ratio of posterior pituitary signal intensity = average gray value of the posterior pituitary/average gray value of pons. The ratio of posterior pituitary signal intensity > 1.00 was defined as a high signal, and ≤1.00 was a high signal loss or decrease. Children with CDI showed high signal loss in the posterior pituitary or a significant reduction in high signal volume.

(3) Evaluation of Pituitary Stalk Morphology. The morphology of the pituitary stalk, saddle area, and parasellar structures was observed. Pituitary stalks could be classified to be blocked, normal, and thickened depending on the morphology.

Pituitary stalk block, including pituitary stalk absent and pituitary stalk sessile, was generally assessed by thin-section MRI and clinically known as pituitary stalk block syndrome. Our MRI classification of blockade [9] was mainly based on whether it was divided into two consecutive stages: the pituitary stalk was partially blocked and could be displayed on MRI images, but it was represented by a slender pituitary stalk with or without pituitary ectopic position or missing, mostly accompanied by anterior pituitary dysplasia (the anterior pituitary volume became smaller, and the height was less than 1 standard deviation of the same age group or more); this condition was called partial blockade; the pituitary stalk was completely blocked. The pituitary stalks on the MRI image cannot be displayed, or display was interrupted. The ectopic or absent posterior pituitary and the anterior pituitary hypoplasia (same as before) were called complete blockade.

Tien et al. [10] suggested that the upper limit of the pituitary stalk was 3.5 mm on the pituitary MRI, and the pituitary stalk was thickened if it exceeded this limit. Elster et al. [11] reported that the pituitary stalk may be enlarged when pregnant but no more than 4 mm. We combined the literature to divide the thickening of the pituitary stalk into mild, moderate, and severe degrees according to the degree of thickness [12], of which the slightest thickening was the maximum transverse diameter of the pituitary stalk 3.0-4.5 mm, and the medium thickening was that the maximum transverse diameter in the pituitary stalk was 4.6-6.5 mm, and severe thickening was that the maximum transverse diameter in the pituitary stalk was 6.5 mm or more.

2.9. Statistical Analysis. All data were analyzed by using SPSS 17.0 statistical software (SPSS Inc., Chicago, IL, U.S.). The results were expressed as the mean ± standard deviation

(SD). The count data were statistically compared using the χ^2 test. The measurement data were statistically compared using the independent sample design t-test. A P value of less than 0.05 was considered as statistically significant.

3. Results

3.1. Clinical Features of CDI Patients. Seventy-nine CDI patients eligible for the criteria were included in the study, 53 male and 26 female. The onset age was ranged from 12 months to 15 years, and the disease duration was ranged from 7 months to 9 years. All patients had no family history of CDI, and 25 patients had a history of central nervous system surgery for more than 3 months. The most common symptoms were polydipsia and polyuria in all patients. Seven patients experienced progressive vision loss, loss of vision, paroxysmal headache, and other nonspecific symptoms with mild polydipsia and polyuria. Other symptoms appeared, such as increased nocturia and bedwetting (75 cases), breast and vulvar development (11 cases), short stature (44 cases), anorexia (63 cases), vomiting (25 cases), headache (3 cases), rash (2 cases), emaciation (10 cases), mental retardation (2 cases), and abnormal walking (1 case). All patients were confirmed as having CDI by the water deprivation vasopressin test and MRI of the pituitary area.

3.2. Etiological Classification of CDI. Of the 79 children with CDI, 25 (15 male and 10 female, aged 4-13 years with a median age of 8 years) had craniopharyngioma surgery (ameloblastoma type) more than 3 months after operation. Three cases (12%) were diagnosed with CDI before craniopharyngioma surgery (Figures 1(a) and 1(b)), 20 cases (80%) after craniopharyngioma surgery, accompanied by 3-5 anterior pituitary functions. Before and after radiotherapy for germ cell tumors, 17 cases with intracranial germ cell tumors (icGCT) were followed up, and the pituitary MRI showed that 7 cases were located in the saddle region and the pineal region (Figures 1(c) and 1(d)), and 3 cases were located in the saddle region. The thickening of pituitary stalks disappeared in 7 cases and was rapidly increased during follow-up; tumor markers and postradiotherapy response confirmed icGCT. The levels of β-HCG were increased in 4 patients with polydipsia, polyuria, and dwarfism, and the levels of β-HCG increased in 4 icGCT patients with polydipsia, polyuria, weight loss, and vomiting. The levels of IGF-1 in 5 cases (29.4%) were decreased, 6 cases (35.3%) showed hypopituitary-thyroid dysfunction, 4 cases (23.5%) appeared to have low secondary cortisol, 2 cases (11.8%) experienced an increase in stress cortisol, 2 cases were treated with surgery, 14 (82.4%) icGCT were sensitive to radiotherapy, and tumors disappeared or nearly disappeared. Eleven cases (64.7%) had 1-5 types of hypopituitarism. Two patients have Langerhans cell histiocytosis (Figures 1(e) and 1(f)), and 33 cases have pituitary stalk interruption syndrome (PSIS). PSIS is a congenital abnormality of the pituitary gland responsible for pituitary deficiency, characterized by the triad of a thin or interrupted pituitary stalk, an ectopic posterior pituitary, and hypoplasia or aplasia of the anterior pituitary on MRI. Pituitary MRI showed that anterior pituitary atrophy, pituitary stalk disruption, and high signal of posterior pituitary disappeared in 30 cases. Ectopic posterior pituitary nearly disappeared in 3 cases, and idiopathic CDI in 2 cases. The pituitary stalk was slightly thickened, and the posterior pituitary gland disappeared. The coagulation treatment was performed and followed up once every 3 months. The pituitary MRI was initially reviewed once every 3 months and reviewed once in the second half of the year. The pituitary stalk returned to normal after 2-year follow-up. Therefore, it was considered as idiopathic CDI.

3.3. Water Deprivation Vasopressin Test. The 24 h urine volume of 79 patients was 202.7 ± 9.83 ml/kg. Specific data of water deprivation vasopressin test are shown in Table 2. The urine loss of all patients was not significantly reduced after water deprivation, urine specific gravity and urine osmotic pressure were not significantly increased (all $P > 0.05$), and serum sodium and osmotic pressure were significantly increased (both $P < 0.05$). After subcutaneous injection of vasopressin aqueous solution in posterior pituitary, urine volume was evidently decreased, urine specific gravity and urine osmotic pressure were considerably increased, and serum sodium and osmotic pressure were dramatically decreased (all $P < 0.05$).

3.4. Comparison of MRI Findings between CDI and Control Groups. No significant difference was noted in age and gender between the two groups. However, height and body mass index (BMI) in the CDI group were lower than those in the control group. The 24 h urine volume was higher in the CDI group than in the control group (Table 3). Of these, 44/79 cases (55.6%) were eligible for the criteria for dwarfism.

The ratio of the posterior pituitary signal intensity was 1.68 ± 0.25 in the control group and 0.88 ± 0.21 in the CDI group. The high signals of the posterior pituitary in CDI patients almost disappeared or were decreased (Figure 2), and most of the signals were low signals relative to the pons. The pituitary volume was roughly represented by the pituitary height, width, and front-rear diameter (mm^3). The pituitary volume in 43 patients was 320.8 ± 64.5 mm^3 in the control group; 35 patients in the CDI group have 160.2 ± 30.4 mm^3. The pituitary volume of 33/35 cases (94.3%) of patients with CDI had different degrees that became smaller ($P < 0.01$).

In 79 patients, except for 25 cases after craniopharyngioma surgery, pituitary iccCT in the saddle area could not be identified in 11 cases, and pituitary stalk abnormalities were found in 44 cases, among which 33 cases of PSIS patients had complete occlusion of the pituitary stalk, and 3 cases were partially blocked (Figure 3). Pituitary stalks in 11 cases (two cases were slightly thickened and were confirmed as idiopathic CDI after long-term follow-up, 5 cases were moderately thickened, and 4 cases were severely thickened) were thickened to varying degrees. As for 9 cases with severe thickening of the pituitary stalk, 7 cases showed rapid growth and multiple pituitary hormone deficiencies (MPHD), whose tumor markers were positive and tumors disappeared after radiotherapy and confirmed as germ cell tumor. Two cases

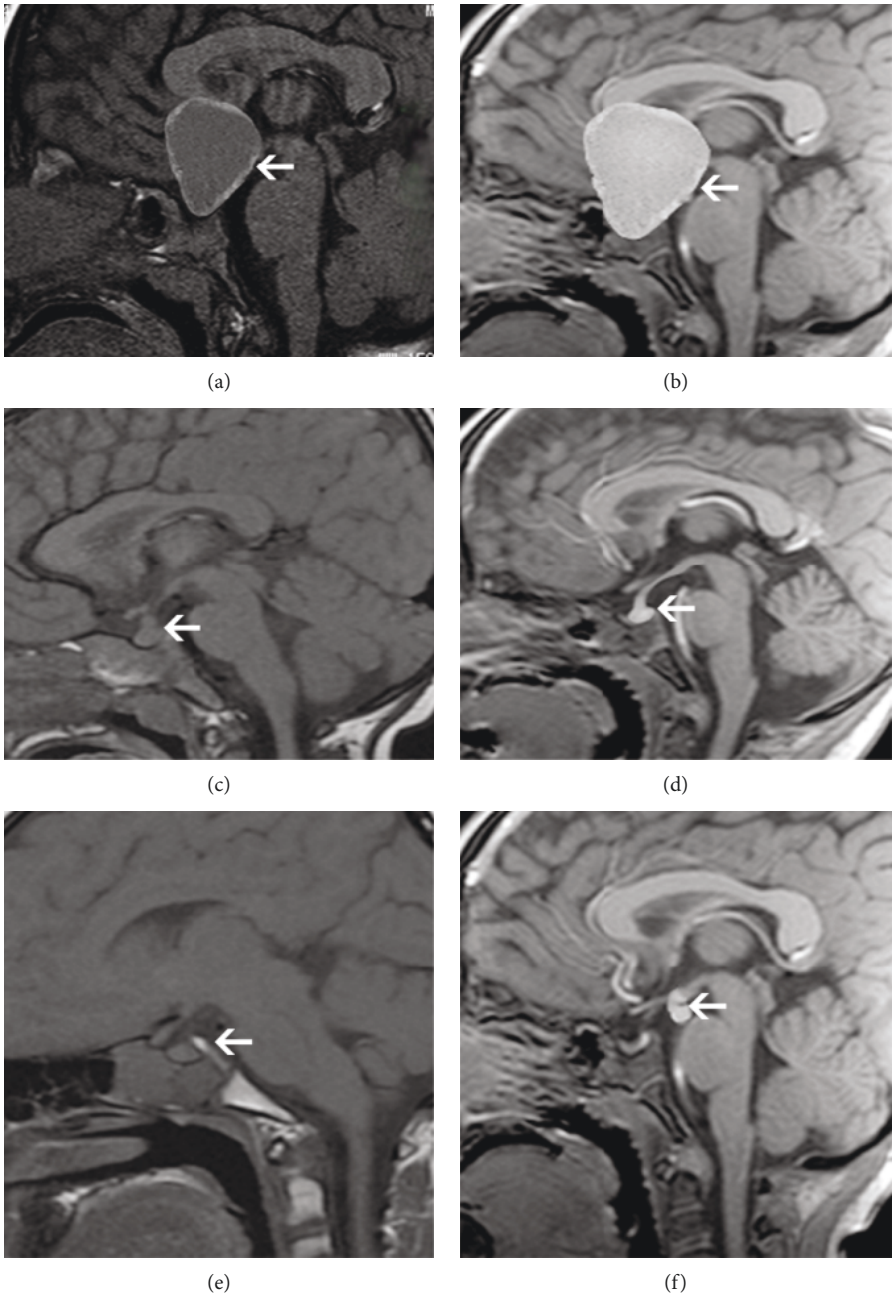

Figure 1: Etiological classification of CDI. Craniopharyngioma: (a) T1WI image showed tumor (white arrowhead); (b) 3D examination showed clearer uniform tumor (white arrow). Intracranial germinoma: (c) T1WI image showed that the upper edge of the pituitary was uplifted, and the posterior high signal was not shown, and the pituitary stalk was thickened (white arrow); (d) the enhanced examination showed that the pituitary stalk and pineal gland were uniformly nodular (white arrows). Langerhans cell histiocytosis: (e) T1WI showed a thickening of the pituitary stalk, showing T1 and other T2 signals, clear edges, pressure in the third ventricle, disappearance of the funnel crypt, slightly increased pressure in the optic chiasm, and no signal in the posterior pituitary; (f) the enhanced scan showed mild even enhancement of the mass, and the anterior pituitary was less clear.

were diagnosed with skull defects, confirmed as Langerhans cell histiocytosis by pathological examination. The pituitary stalk thickening was reduced after chemotherapy, but polydipsia and polyuria should be properly controlled.

3.5. MRI Changes of CDI Complicated with Hypopituitarism. The abnormalities of hormone secretion in the anterior pituitary were found in 44 cases upon the initial diagnosis (Table 4). The anterior leaf volume of 33 patients with MPHD was significantly smaller compared with that of the patients with IGHD ($P < 0.05$). All 44 patients with short stature had growth hormone deficiency, and 2 patients with mental retardation experienced MPHD. As shown in Table 5, 7 cases with moderate-severe pituitary stalk thickening developed into icGCT in the follow-up and appeared as MPHD, and 33 PSIS patients with CDI had MPHD.

Table 2: Results of water deprivation and vasopressin test in patients with CID.

	Blood Na^+ (mmol/l)	Blood osmotic pressure (mOsm/kg)	Urinary osmotic pressure (mOsm/kg)	Urine specific gravity
Before water deprivation	144.3 ± 10.9	286.2 ± 15.6	128.6 ± 6.8	1.00-1.004
After water deprivation	156.0 ± 15.2*	307.5 ± 20.9*	179.1 ± 10.5	1.00-1.010*
After injection of vasopressin	142.9 ± 8.8*	278.7 ± 11.3*	602 ± 58.6*	1.01-1.028*

*$P < 0.05$.

Table 3: Comparison between baseline data of CDI and control groups.

	CDI group ($n = 79$)	Control group ($n = 43$)	P
Male/female	53/26	28/15	>0.05
Age	7.60 ± 2.49	7.45 ± 1.96	>0.05
Height (mean ± standard deviation)	-3.23 ± 1.24	0.68 ± 0.35	<0.01
BMI	14.12 ± 2.56	18.28 ± 3.32	<0.05
24 h urine volume (ml/kg)	202.7 ± 9.83	88.6 ± 12.99	<0.01

4. Discussion

Recent studies found that DI was due to hypothalamic-neuronal lesions caused by the lack of different levels of antidiuretic hormone (ADH) or due to kidney sensitivity to AVP deficiency caused by a variety of lesions [13, 14]. In pediatric CDI, etiology diagnosis and pituitary function monitoring are usually delayed [15]. If the diagnosis and treatment of DI is not timely, it will affect the growth and development of children; it will also affect the study and work efficiency of adults, reduce the quality of life, and cause damage to kidney function. Therefore, for CDI, it is necessary to make a clear diagnosis classification, find the cause, and undergo timely symptomatic treatment.

Clinical manifestations of CDI include polydipsia induced by lack of AVP. As for a vast majority of patients, polydipsia is the first symptom, and 79 cases presented with polydipsia in this study. Most patients initially had increased initial frequency of urination and increased urine output, followed by polydipsia. In children with onset of illness, the bladder, ureters, and pelvis may dilate due to prolonged polyuria, impairing kidney function and possibly develop osteoporosis. Children may have nocturia and bedwetting in this study. If the patient is unable to drink water, hypovolemia can occur, such as palpitations, decreased blood pressure, cold extremities, shock, and prerenal azotemia, and timely supplementation of blood volume can be promptly corrected. If the hypovolemic state cannot be corrected promptly, headaches, irritability, hopelessness, and coma can occur. Others included 11 cases with breast and exogenous development. Most children with CDI had digestive symptoms, vomiting and poor appetite. In this study, 63 cases presented with anorexia, 25 cases with vomiting, and 10 cases with weight loss, and CDI patients may be complicated with hypopituitary dysfunction, which may affect the growth and development of children. In this study, 44 cases experienced short stature, and 2 cases suffered from mental retardation.

GH and GnRH deficiencies often occur before the anterior pituitary hormone deficiency, subsequently followed by TSH and ACTH deficiency [16, 17]. For 79 CDI patients in this study, 44 cases had hypopituitary dysfunction, and all presented with GH deficiency. Among them, 33 cases had two or more hormone deficiencies, 33 cases had secondary hypothyroidism, and 20 cases had hypogonadism. 30 children had secondary adrenal insufficiency, 33 cases had elevated PRL, and 11 cases had reduced PRL, indicating that CDI patients had a variety of endocrine gland secretion abnormalities. Insufficient secretion of hormones in the anterior pituitary gland will produce a series of symptoms and signs of corresponding target gland dysfunction, and its severity is related to the degree of hormone deficiency. This study also found that the pituitary volume of the CDI group was smaller than that of the control group, indicating that when hypothalamic-nerve pituitary system lesions occurred, it not only induced ADH deficiency to cause DI but also induced pituitary anterior pituitary dysfunction. And 44 patients with hypopituitarism in the pituitary gland had organic lesions. Among them, 44 patients with short stature had GH deficiency, and 2 patients with mental retardation also had MPHD. Therefore, patients with CDI needed to pay close attention to the anterior pituitary secretion to actively remove the cause or perform symptomatic treatment and to avoid serious consequences such as short stature and delayed mental development.

When the morphological changes (such as interruption, tumor compression, infiltration, and destruction) of pituitary stalk occur, it can cause the downward transport channel of the pituitary hormone to be blocked, possibly leading to the occurrence of pituitary hypofunction. Biopsy should be performed when the pituitary stalk thickens >6.5 mm to determine the specific cause [18]. Germ cell tumors contain large epithelial cells and small lymphocytes pathologically. They are very sensitive to radiotherapy and chemotherapy and are a curable tumor [19]. When the site of lesion growth is special and difficult to take biopsy, germ cell tumor can be diagnosed based on patient's medical history, serum or cerebrospinal fluid tumor marker detection, and germ cell tumor sensitivity to radiotherapy and chemotherapy [20]. Our study found that 44 CDI patients with anterior pituitary hypothyroidism had pituitary stalk morphological changes, 33 cases showed pituitary stalk block, and 11 cases presented with the thickening of the pituitary stalk. When the pituitary stalk was significantly thickened, the pituitary stalk pathway

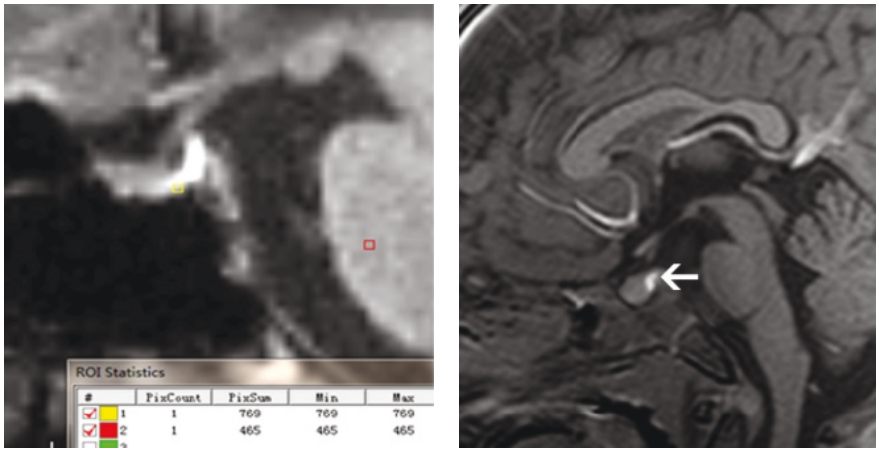

(a) (b)

Figure 2: Measurement of the posterior pituitary signal intensity. (a) The signal intensity of the posterior pituitary of the normal pituitary was higher than that of the pons. (b) The high signal of the posterior pituitary (white arrow) contrasts with the anterior pituitary and the pons.

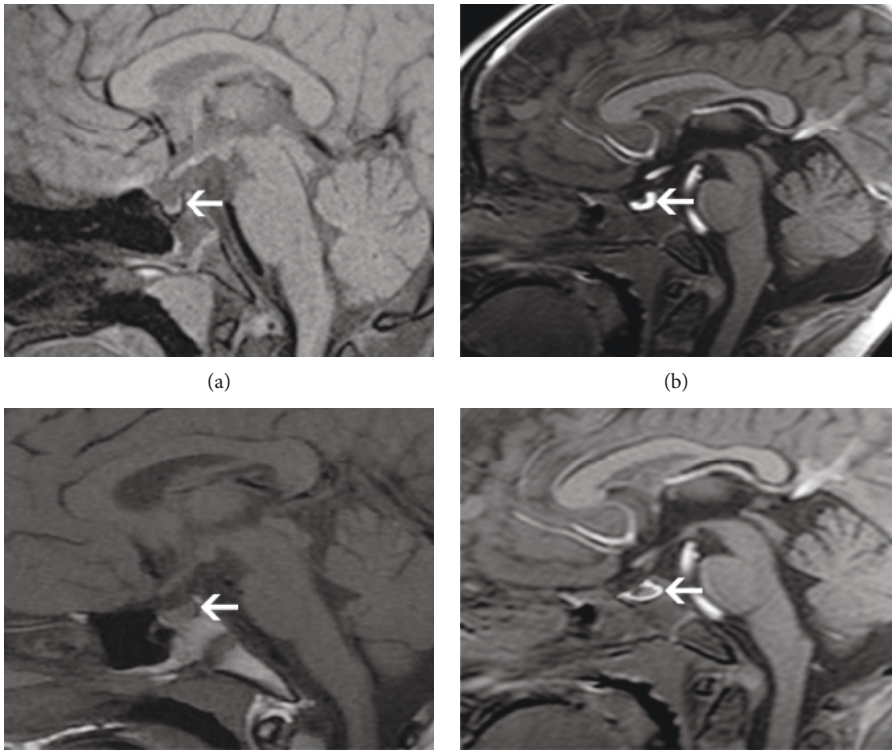

(a) (b)

(c) (d)

Figure 3: Pituitary stem blockage syndrome. (a) T1WI showed that the anterior pituitary was thin, the central site was sunken, the posterior pituitary high signal was not clearly shown, and the pituitary stalk was interrupted (white arrow). (b) The enhanced examination showed a small ectopic position in the anterior pituitary and after the optic chiasm, and obvious uniform enhancement was found in the posterior leaves. (c) T1WI showed that high intensity of posterior pituitary was disappeared and the pituitary stalk showed a thin line. (d) The enhanced examination showed anterior pituitary atrophy.

will be seriously blocked, or when the hypothalamus was under pressure and invasion, the anterior pituitary gland cannot absorb sufficient nutrition and regulation, resulting in low secretion function, atrophy, and lack of a variety of pituitary hormone secretion. The pituitary stalk was severely thickened in 7 cases with sellar region germ cell tumors complicated with MPHD. 2 LCH children also showed severe thickening of the pituitary stalk with MPHD. 2 cases with idiopathic CDI in children showed mild thickening of the pituitary stalk.

Studies have shown that CDI is also an autoimmune disease [21–23]. Study found that autoreactive CD8+ T cells can

Table 4: Relationship of abnormal hormone secretion in the anterior pituitary with pituitary volume and patient development.

	Number	Pituitary volume		Short stature	Mental retardation
		Smaller	Normal		
IGHD	11	5	6	11	0
MPHD	33	33	0	33	2

Table 5: Relationship of pituitary stalk abnormalities with anterior pituitary hormone secretion abnormalities.

Pituitary stalk form	Number	Anterior pituitary hormone		MPHD
		Normal	Deficiency	
Mild thickening	2	2	0	0
Moderate-severe thickening	9	2	7	7
Partially blocked	3	0	3	3
Completely blocked	30	0	30	30

attack CNS neurons, leading to CDI [24], suggesting that immunotherapy interventions or inhibition of the inflammatory response mediated by the immune system could be used for the treatment of CDI. Previous study has found that a small number of CDI had a family history of antidiuretic hormone due to gene mutation of antidiuretic hormone-posterior leaf hormone transporter (AVP-NPII) [25].

In conclusion, the high signal intensity of the posterior lobe and the pituitary stalk is clearly displayed on T1WI-3D MP RAGE images. The signal intensity ratio of the posterior lobe, the measurement of pituitary volume, and the morphology assessment of pituitary stalk on T1WI-3D MP RAGE images contribute to the diagnosis of CDI. The thickening of the pituitary stalk in patients with CDI should be subject to long-term follow-up. In addition, the detection of tumor biomarkers, such as beta-HCG, plays a role in identifying the etiology of CDI. The premature outcomes in this study remain to be validated by subsequent investigations, such as antibody detection experiment.

Data Availability

The data used to support the findings of this study are available from the corresponding author upon request.

Conflicts of Interest

The authors declare that there is no conflict of interest regarding the publication of this paper.

Acknowledgments

The authors are grateful to all the children and their parents for participating in this study.

References

[1] M. L. Moritz and J. C. Ayus, "Diabetes insipidus and syndrome of inappropriate antidiuretic hormone," in *Textbook of Nephro-Endocrinology*, pp. 133–161, Academic Press, 2018.

[2] H. Arima, Y. Azuma, Y. Morishita, and D. Hagiwara, *Central Diabetes Insipidus*, Springer, Berlin Heidelberg, 2016.

[3] R. Barry, A. O' Connor, M. H. Awang, and O. O' Toole, "'If there were water we should stop and drink': neurofibromatosis presenting with diabetes insipidus," *BML Case Reports*, vol. 2018, 2018.

[4] A. León-Suárez, P. Roldán-Sarmiento, M. A. Gómez-Sámano et al., "Infundibulo-hypophysitis-like radiological image in a patient with pituitary infiltration of a diffuse large B-cell non-Hodgkin lymphoma," *Endocrinology, Diabetes & Metabolism Case Reports*, vol. 2016, p. 2016, 2016.

[5] I. Lazzari, A. Graziani, F. Mirici, and G. F. Stefanini, "Transient idiopathic central diabetes insipidus: is severe sepsis a possible cause?," *Italian Journal of Medicine*, vol. 11, no. 1, p. 78, 2017.

[6] J. E. Park, Y. H. Choi, J. E. Cheon et al., "Three-dimensional radial VIBE sequence for contrast-enhanced brain imaging: an alternative for reducing motion artifacts in restless children," *American Journal of Roentgenology*, vol. 210, no. 4, pp. 876–882, 2018.

[7] Y. Yang, F. Jia, W. T. Siok, and L. H. Tan, "Altered functional connectivity in persistent developmental stuttering," *Scientific Reports*, vol. 6, no. 1, article 19128, 2016.

[8] R. Deichmann, C. D. Good, O. Josephs, J. Ashburner, and R. Turner, "Optimization of 3-D MP-RAGE sequences for structural brain imaging," *NeuroImage*, vol. 12, no. 1, pp. 112–127, 2000.

[9] J. Hamilton, S. Blaser, and D. Daneman, "MR imaging in idiopathic growth hormone deficiency," *American Journal of Neuroradiology*, vol. 19, no. 9, pp. 1609–1615, 1998.

[10] R. D. Tien, T. H. Newton, M. W. Mcdermott, W. P. Dillon, and J. Kucharczyk, "Thickened pituitary stalk on MR images in patients with diabetes insipidus and Langerhans cell histiocytosis," *American Journal of Neuroradiology*, vol. 11, no. 4, pp. 703–708, 1990.

[11] A. D. Elster, T. G. Sanders, F. S. Vines, and M. Y. Chen, "Size and shape of the pituitary gland during pregnancy and post partum: measurement with MR imaging," *Radiology*, vol. 181, no. 2, pp. 531–535, 1991.

[12] P. Czernichow, C. Garel, and J. Léger, "Thickened pituitary stalk on magnetic resonance imaging in children with central diabetes insipidus," *Hormone Research in Pædiatrics*, vol. 53, no. 3, pp. 61–64, 2000.

[13] F. Qari, E. AbuDaood, and T. Nasser, "Diabetes insipidus following neurosurgery at a university hospital in Western Saudi Arabia," *Saudi Medical Journal*, vol. 37, no. 2, pp. 156–160, 2016.

[14] S. Milano, M. Carmosino, A. Gerbino, M. Svelto, and G. Procino, "Hereditary nephrogenic diabetes insipidus: pathophysiology and possible treatment. An update," *International Journal of Molecular Sciences*, vol. 18, no. 11, p. 2385, 2017.

[15] W. Liu, L. Wang, M. Liu, and G. Li, "Pituitary morphology and function in 43 children with central diabetes insipidus," *International Journal of Endocrinology*, vol. 2016, Article ID 6365830, 7 pages, 2016.

[16] M. Cerbone and M. T. Dattani, "Progression from isolated growth hormone deficiency to combined pituitary hormone

deficiency," *Growth Hormone & IGF Research*, vol. 37, pp. 19–25, 2017.

[17] A. Jannin, E. Merlen, C. Do Cao, and N. Penel, "L'hypophysite auto-immune, complication des nouvelles immunothérapies anticancéreuses," *Bulletin du Cancer*, vol. 105, no. 3, pp. 275–280, 2018.

[18] A. E. Al-Agha, M. J. Thomsett, J. F. Ratcliffe, A. M. Cotterill, and J. A. Batch, "Acquired central diabetes insipidus in children: a 12-year Brisbane experience," *Journal of Paediatrics and Child Health*, vol. 37, no. 2, pp. 172–175, 2001.

[19] W. G. Breen, M. J. Blanchard, A. N. Rao, D. J. Daniels, J. C. Buckner, and N. N. I. Laack, "Optimal radiotherapy target volumes in intracranial nongerminomatous germ cell tumors: long-term institutional experience with chemotherapy, surgery, and dose- and field-adapted radiotherapy," *Pediatric Blood & Cancer*, vol. 64, no. 11, article e26637, 2017.

[20] Y. Shibamoto, M. Takahashi, and K. Sasai, "Prognosis of intracranial germinoma with syncytiotrophoblastic giant cells treated by radiation therapy," *International Journal of Radiation Oncology Biology Physics*, vol. 37, no. 3, pp. 505–510, 1997.

[21] M. J. Hannon, C. Orr, C. Moran et al., "Anterior hypopituitarism is rare and autoimmune disease is common in adults with idiopathic central diabetes insipidus," *Clinical Endocrinology*, vol. 76, no. 5, pp. 725–728, 2012.

[22] G. Murdaca, R. Russo, F. Spanò et al., "Autoimmune central diabetes insipidus in a patient with ureaplasma urealyticum infection and review on new triggers of immune response," *Archives of Endocrinology and Metabolism*, vol. 59, no. 6, pp. 554–558, 2015.

[23] G. Bellastella, A. Bizzarro, E. Aitella et al., "Pregnancy may favour the development of severe autoimmune central diabetes insipidus in women with vasopressin cell antibodies: description of two cases," *European Journal of Endocrinology*, vol. 172, no. 3, pp. K11–K17, 2015.

[24] T. Scheikl, B. Pignolet, C. Dalard et al., "Cutting edge: neuronal recognition by CD8 T cells elicits central diabetes insipidus," *The Journal of Immunology*, vol. 188, no. 10, pp. 4731–4735, 2012.

[25] S. Ghirardello, C. Malattia, P. Scagnelli, and M. Maghnie, "Current perspective on the pathogenesis of central diabetes insipidus," *Journal of Pediatric Endocrinology and Metabolism*, vol. 18, no. 7, pp. 631–645, 2005.